Chapter 4

FEYNMAN DIAGRAMS EXPANSION IN FERROMAGNETS

4.1. Temperature Green Function and Perturbation Expansion

We have seen in Eq. (3.2.17) that the neutron scattering cross-section may be written in terms of the generalized boson Green function $G_{\boldsymbol{k}}(\omega \pm i\epsilon)$ solution of the equation of motion given by Eq. (3.2.19). In the diagram expansion, it is more convenient to define the *temperature Green function*[13]

$$\mathcal{G}_{\boldsymbol{k}}(\tau) = -\langle T[a^{\mathrm{H}}_{\boldsymbol{k}}(\tau)a^{+}_{\boldsymbol{k}}]\rangle \tag{4.1.1}$$

where $\tau = it$ is an imaginary time and T is the ordering time operator that puts the operators within the square brakets in such a way that the time decreases going from the first to the last. In particular, for $\tau > 0$, the temperature Green function (4.1.1) reduces to $\mathcal{G}_{\boldsymbol{k}}(\tau) = -\langle a^{\mathrm{H}}_{\boldsymbol{k}}(\tau)a^{+}_{\boldsymbol{k}}\rangle$. The "time evolution" of the boson operator in the Heisenberg picture is given by

$$a^{\mathrm{H}}_{\boldsymbol{k}}(\tau) = e^{\mathcal{H}\tau/\hbar}a_{\boldsymbol{k}}e^{-\mathcal{H}\tau/\hbar} \tag{4.1.2}$$

where

$$\mathcal{H} = \mathcal{H}_0 + \mathcal{H}_{\mathrm{int}} \tag{4.1.3}$$

with

$$\mathcal{H}_0 = \sum_{\boldsymbol{q}} \hbar\omega_{\boldsymbol{q}} a^{+}_{\boldsymbol{q}} a_{\boldsymbol{q}}, \quad \hbar\omega_{\boldsymbol{q}} = 2zJS(1-\gamma_{\boldsymbol{q}}), \tag{4.1.4}$$

$$\mathcal{H}_{\mathrm{int}} = \sum_{\boldsymbol{q}_1,\boldsymbol{q}_2,\boldsymbol{q}_3,\boldsymbol{q}_4} V_{\boldsymbol{q}_1,\boldsymbol{q}_2,\boldsymbol{q}_3,\boldsymbol{q}_4} a^{+}_{\boldsymbol{q}_1} a^{+}_{\boldsymbol{q}_2} a_{\boldsymbol{q}_3} a_{\boldsymbol{q}_4} \tag{4.1.5}$$

and

$$V_{\boldsymbol{q}_1,\boldsymbol{q}_2,\boldsymbol{q}_3,\boldsymbol{q}_4} = -\frac{zJ}{N}\delta_{\boldsymbol{q}_1+\boldsymbol{q}_2,\boldsymbol{q}_3+\boldsymbol{q}_4} v_{\boldsymbol{q}_1,\boldsymbol{q}_2,\boldsymbol{q}_3,\boldsymbol{q}_4} \tag{4.1.6a}$$

where

$$v_{\boldsymbol{q}_1,\boldsymbol{q}_2,\boldsymbol{q}_3,\boldsymbol{q}_4} = \frac{1}{4}\left(\gamma_{\boldsymbol{q}_1-\boldsymbol{q}_3} + \gamma_{\boldsymbol{q}_1-\boldsymbol{q}_4} + \gamma_{\boldsymbol{q}_2-\boldsymbol{q}_3} + \gamma_{\boldsymbol{q}_2-\boldsymbol{q}_4}\right) - \frac{1}{2}\left(\gamma_{\boldsymbol{q}_1} + \gamma_{\boldsymbol{q}_2}\right) \quad (4.1.6b)$$

is the DM interaction potential. Now, we intend to illustrate the main steps to arrive at a perturbation expansion for the temperature Green function. Let us begin by introducing the "interaction picture" in which the time dependent operators evolve according to the non-interacting Hamiltonian $\mathcal{H}_0$ that is

$$a_{\boldsymbol{k}}(\tau) = e^{\mathcal{H}_0\tau/\hbar} a_{\boldsymbol{k}} e^{-\mathcal{H}_0\tau/\hbar}. \quad (4.1.7)$$

The interaction picture is particularly convenient in view of a perturbative expansion since the unperturbed Hamiltonian is involved. However, since in the temperature Green function of Eq. (4.1.1), the time evolution is ruled by the full Hamiltonian (Heisenberg picture), the relationship between the Heisenberg and the interaction picture becomes of fundamental importance. From Eqs. (4.1.2) and (4.1.7), one obtains

$$a^{\mathrm{H}}_{\boldsymbol{k}}(\tau) = e^{\mathcal{H}\tau/\hbar} e^{-\mathcal{H}_0\tau/\hbar} a_{\boldsymbol{k}}(\tau) e^{\mathcal{H}_0\tau/\hbar} e^{-\mathcal{H}\tau/\hbar} = \mathcal{U}(0,\tau) a_{\boldsymbol{k}}(\tau) \mathcal{U}(\tau,0) \quad (4.1.8)$$

where

$$\mathcal{U}(\tau,\tau') = e^{\mathcal{H}_0\tau/\hbar} e^{-\mathcal{H}(\tau-\tau')/\hbar} e^{-\mathcal{H}_0\tau'/\hbar}. \quad (4.1.9)$$

From Eq. (4.1.9), one has

$$\mathcal{U}(\tau,\tau) = 1 \quad (4.1.9a)$$

and

$$\mathcal{U}(\beta\hbar,0) = e^{\beta\mathcal{H}_0} e^{-\beta\mathcal{H}}. \quad (4.1.9b)$$

The time derivative of $\mathcal{U}(\tau,\tau')$ with respect to τ leads to the integral-differential equation

$$\mathcal{U}(\tau,\tau') = 1 - \frac{1}{\hbar}\int_{\tau'}^{\tau} \mathcal{H}_{\mathrm{int}}(\tau'')\mathcal{U}(\tau'',\tau')d\tau'' \quad (4.1.10)$$

where

$$\mathcal{H}_{\mathrm{int}}(\tau'') = e^{\mathcal{H}_0\tau''/\hbar} \mathcal{H}_{\mathrm{int}} e^{-\mathcal{H}_0\tau''/\hbar}. \quad (4.1.11)$$

The iterative solution of Eq. (4.1.11) is given by[13]

$$\mathcal{U}(\tau,\tau') = \sum_{n=0}^{\infty} \left(-\frac{1}{\hbar}\right)^n \frac{1}{n!} \int_{\tau'}^{\tau} d\tau_1 \cdots \int_{\tau'}^{\tau} d\tau_n T[\mathcal{H}_{\mathrm{int}}(\tau_1)\cdots\mathcal{H}_{\mathrm{int}}(\tau_n)] \quad (4.1.12)$$

where the time ordering operator is due to the fact that the interaction Hamiltonians $\mathcal{H}_{\mathrm{int}}$ do not commute at different times. By means of Eq. (4.1.9b), one may write

the granpartition funtion as

$$\mathcal{Q} = \mathrm{Tr}(e^{-\beta\mathcal{H}}) = \mathrm{Tr}[e^{-\beta\mathcal{H}_0}\mathcal{U}(\beta\hbar, 0)] \tag{4.1.13}$$

and using Eq. (4.1.12), one obtains

$$\mathcal{Q} = \mathrm{Tr}(e^{-\beta\mathcal{H}_0}) \sum_{n=0}^{\infty} \left(-\frac{1}{\hbar}\right)^n \frac{1}{n!} \int_0^{\beta\hbar} d\tau_1 \cdots \int_0^{\beta\hbar} d\tau_n \, \langle T[\mathcal{H}_{\mathrm{int}}(\tau_1) \cdots \mathcal{H}_{\mathrm{int}}(\tau_n)]\rangle_0 \tag{4.1.14}$$

where

$$\langle \mathcal{O} \rangle_0 = \frac{\mathrm{Tr}(\mathcal{O} e^{-\beta\mathcal{H}_0})}{\mathrm{Tr}(e^{-\beta\mathcal{H}_0})}. \tag{4.1.15}$$

By means of the relationship[13]

$$\mathcal{U}(\beta\hbar, \tau) a_{\boldsymbol{k}}(\tau) \mathcal{U}(\tau, 0) = \sum_{n=0}^{\infty} \left(-\frac{1}{\hbar}\right)^n \frac{1}{n!} \int_0^{\beta\hbar} d\tau_1 \cdots \times \int_0^{\beta\hbar} d\tau_n \langle T[\mathcal{H}_{\mathrm{int}}(\tau_1) \cdots \mathcal{H}_{\mathrm{int}}(\tau_n) a_{\boldsymbol{k}}(\tau)]\rangle_0 \tag{4.1.16}$$

and of Eqs. (4.1.8), (4.1.14) and (4.1.16), the temperature Green function (4.1.1) becomes

$$\begin{aligned} \mathcal{G}_{\boldsymbol{k}}(\tau) &= -\frac{1}{\mathcal{Q}} \mathrm{Tr}[e^{-\beta\mathcal{H}_0} \mathcal{U}(\beta\hbar, \tau) a_{\boldsymbol{k}}(\tau) \mathcal{U}(\tau, 0) a_{\boldsymbol{k}}^+] \\ &= -\frac{\sum_{n=0}^{\infty} \left(-\frac{1}{\hbar}\right)^n \frac{1}{n!} \int_0^{\beta\hbar} d\tau_1 \cdots \int_0^{\beta\hbar} d\tau_n \langle T[\mathcal{H}_{\mathrm{int}}(\tau_1) \cdots \mathcal{H}_{\mathrm{int}}(\tau_n) a_{\boldsymbol{k}}(\tau) a_{\boldsymbol{k}}^+]\rangle_0}{\sum_{n=0}^{\infty} \left(-\frac{1}{\hbar}\right)^n \frac{1}{n!} \int_0^{\beta\hbar} d\tau_1 \cdots \int_0^{\beta\hbar} d\tau_n \langle T[\mathcal{H}_{\mathrm{int}}(\tau_1) \cdots \mathcal{H}_{\mathrm{int}}(\tau_n)]\rangle_0}. \end{aligned} \tag{4.1.17}$$

From Eq. (4.1.5), one realizes that the n-th term in the numerator of Eq. (4.1.17) consists of a time ordered product containing $(2n+1)$ creation and $(2n+1)$ destruction Bose operators while the n-th term in the denominator consists of a time ordered product containing $2n$ creation and $2n$ destruction Bose operators.

Two very important theorems of the many-body theory are used to greatly simplify the series expansions of Eq. (4.1.17). The first theorem is the "generalized Wick's theorem"[13,32] proved by Matsubara:[33] such a theorem, applied to the numerator of Eq. (4.1.17), establishes that the average of a time ordered product containing $(2n+1)$ creation and $(2n+1)$ destruction operators is equal to the sum of $(2n+1)!$ permutations of the fully contracted terms consisting of the product of $(2n+1)$ averages of time ordered products containing one creation and one destruction operator. The second theorem is the "linked cluster theorem"[13,34] that establishes that the series occurring in the numerator of Eq. (4.1.17) can be written as a product of a series containing only "connected diagrams" times a series containing only "disconnected diagrams" which is coincident with the series occurring in the denominator of Eq. (4.1.17). By means of the linked cluster theorem,

Eq. (4.1.17) reduces to

$$\mathcal{G}_{\boldsymbol{k}}(\tau) = -\sum_{n=0}^{\infty}\left(-\frac{1}{\hbar}\right)^n \frac{1}{n!}\int_0^{\beta\hbar} d\tau_1 \cdots \int_0^{\beta\hbar} d\tau_n \langle T[\mathcal{H}_{\rm int}(\tau_1)\cdots\mathcal{H}_{\rm int}(\tau_n)a_{\boldsymbol{k}}(\tau)a_{\boldsymbol{k}}^+]\rangle_0^{\rm c} \tag{4.1.18}$$

where the superscript "c" means that only contributions corresponding to connected diagrams have to be retained in the sum. We will show how to handle Eq. (4.1.18) in the next sections by evaluating explicitly the first few terms of the series expansion. In particular, the zero-order term ($n = 0$) corresponds to the choice $\mathcal{H}_{\rm int} = 0$. Then $\mathcal{H} = \mathcal{H}_0$ and the Heisenberg and interaction pictures coincide so that

$$a_{\boldsymbol{k}}^{\rm H}(\tau) = a_{\boldsymbol{k}}(\tau) = e^{\mathcal{H}_0\tau/\hbar}a_{\boldsymbol{k}}e^{-\mathcal{H}_0\tau/\hbar} = a_{\boldsymbol{k}}e^{-\omega_k\tau}. \tag{4.1.19}$$

The zero-order or "unperturbed" temperature Green function becomes

$$\mathcal{G}_{\boldsymbol{k}}^{(0)}(\tau) = -\langle T[a_{\boldsymbol{k}}(\tau)a_{\boldsymbol{k}}^+]\rangle_0 = \begin{cases} -(1+n_{\boldsymbol{k}}^{(0)})e^{-\omega_k\tau} & \text{for } \tau > 0 \\ -n_{\boldsymbol{k}}^{(0)}e^{-\omega_k\tau} & \text{for } \tau < 0 \end{cases} \tag{4.1.20}$$

where $n_{\boldsymbol{k}}^{(0)} = \langle a_{\boldsymbol{k}}^+ a_{\boldsymbol{k}}\rangle_0 = (e^{\beta\hbar\omega_k} - 1)^{-1}$.

Starting from Eqs. (4.1.1) and (4.1.2), one can prove that the boson temperature Green function $\mathcal{G}_{\boldsymbol{k}}(\tau)$ is a periodic function of τ with period $\beta\hbar$. Indeed, assuming $0 < \tau < \beta\hbar$ and using the cyclic property of the trace, one has

$$\begin{aligned}\mathcal{G}_{\boldsymbol{k}}(\tau) &= -\frac{1}{\mathcal{Q}}{\rm Tr}\left[e^{-\beta\mathcal{H}}e^{\mathcal{H}\tau/\hbar}a_{\boldsymbol{k}}e^{-\mathcal{H}\tau/\hbar}a_{\boldsymbol{k}}^+\right] \\ &= -\frac{1}{\mathcal{Q}}{\rm Tr}\left[a_{\boldsymbol{k}}^+e^{(\tau-\beta\hbar)\mathcal{H}/\hbar}a_{\boldsymbol{k}}e^{-(\tau-\beta\hbar)\mathcal{H}/\hbar}e^{-\beta\mathcal{H}}\right] \\ &= -\frac{1}{\mathcal{Q}}{\rm Tr}\left[e^{-\beta\mathcal{H}}a_{\boldsymbol{k}}^+a_{\boldsymbol{k}}^{\rm H}(\tau-\beta\hbar)\right] = -\left\langle T\left[a_{\boldsymbol{k}}^{\rm H}(\tau-\beta\hbar)a_{\boldsymbol{k}}^+\right]\right\rangle = \mathcal{G}_{\boldsymbol{k}}(\tau-\beta\hbar).\end{aligned} \tag{4.1.21}$$

Since the temperature Green function is a periodic function of τ with a period $\beta\hbar$, it may be expanded in a Fourier series

$$\mathcal{G}_{\boldsymbol{k}}(\tau) = \frac{1}{\beta\hbar}\sum_n e^{-i\omega_n\tau}\mathcal{G}_{\boldsymbol{k}}(i\omega_n) \tag{4.1.22}$$

with

$$\omega_n = \frac{2\pi n}{\beta\hbar} \tag{4.1.23}$$

where the associated Fourier coefficients are given by

$$\mathcal{G}_{\boldsymbol{k}}(i\omega_n) = \int_0^{\beta\hbar} d\tau e^{i\omega_n\tau}\mathcal{G}_{\boldsymbol{k}}(\tau). \tag{4.1.24}$$

For the zero-order temperature Green function (4.1.20), the associated Fourier coefficients given by Eq. (4.1.24) become

$$\mathcal{G}^{(0)}_{\boldsymbol{k}}(i\omega_n) = \int_0^{\beta\hbar} d\tau e^{i\omega_n\tau}\mathcal{G}^{(0)}_{\boldsymbol{k}}(\tau) = -(1+n^{(0)}_{\boldsymbol{k}})\int_0^{\beta\hbar} d\tau e^{(i\omega_n-\omega_{\boldsymbol{k}})\tau}$$
$$= -(1+n^{(0)}_{\boldsymbol{k}})\frac{e^{(i\omega_n-\omega_{\boldsymbol{k}})\beta\hbar}-1}{i\omega_n-\omega_{\boldsymbol{k}}} = \frac{1}{i\omega_n-\omega_{\boldsymbol{k}}}. \tag{4.1.25}$$

The relationship between the temperature Green function (4.1.24) and the generalized Green functions (3.2.10) is easily obtained using Eqs.(4.1.1), (4.1.2), (3.2.6) and (4.1.23). Indeed,

$$\mathcal{G}_{\boldsymbol{k}}(i\omega_n) = -\int_0^{\beta\hbar} d\tau e^{i\omega_n\tau}\frac{1}{\mathcal{Q}}\sum_{\mu,\nu}\langle\mu|a_{\boldsymbol{k}}|\nu\rangle\langle\nu|a^+_{\boldsymbol{k}}|\mu\rangle e^{-\beta E_\mu}e^{(E_\mu-E_\nu)\tau/\hbar}$$
$$= -\int_0^{\beta\hbar} d\tau e^{i\omega_n\tau}\int_{-\infty}^{+\infty} d\omega' e^{-\omega'\tau}e^{\beta\hbar\omega'}J(\omega')$$
$$= \int_{-\infty}^{+\infty} d\omega'\left(e^{\beta\hbar\omega'}-1\right)J(\omega')\frac{1}{i\omega_n-\omega'} = G_{\boldsymbol{k}}(z=i\omega_n). \tag{4.1.26}$$

As one can see from Eq. (4.1.26), the temperature Green function coincides with the generalized Green function (3.2.10) evaluated at $z = i\omega_n$. Therefore, a suitable[13] analytic continuation of the temperature Green function to the complex z-plane recovers the generalized Green function that enters the neutron scattering cross-section.

4.2. First-Order Perturbation Theory

The first-order temperature Green function corresponds to the term with $n = 1$ of the expansion (4.1.18). From now on, we will omit the subscript "0" since all the averages occurring in the series expansion (4.1.18) are performed over the eigenstates of the unperturbed Hamiltonian $\mathcal{H}_0$ (interaction picture) while we keep the label "c" because only connected diagrams have to be retained in the expansion. Then the first-order term of the expansion (4.1.18) reads

$$\mathcal{G}^{(1)}_{\boldsymbol{k}}(\tau) = \frac{1}{\hbar}\int_0^{\beta\hbar} d\tau_1\langle T[\mathcal{H}_{\rm int}(\tau_1)a_{\boldsymbol{k}}(\tau)a^+_{\boldsymbol{k}}]\rangle_{\rm c}$$
$$= \frac{1}{\hbar}\sum_{\boldsymbol{q}_1,\boldsymbol{q}_2,\boldsymbol{q}_3,\boldsymbol{q}_4} V_{\boldsymbol{q}_1,\boldsymbol{q}_2,\boldsymbol{q}_3,\boldsymbol{q}_4}\int_0^{\beta\hbar} d\tau_1\langle T[a^+_{\boldsymbol{q}_1}(\tau_1)a^+_{\boldsymbol{q}_2}(\tau_1)$$
$$\times a_{\boldsymbol{q}_3}(\tau_1)a_{\boldsymbol{q}_4}(\tau_1)a_{\boldsymbol{k}}(\tau)a^+_{\boldsymbol{k}}]\rangle_{\rm c}. \tag{4.2.1}$$

The generalized Wick's theorem[13] applied to the time ordered product of the 3 creation and 3 destruction operators of Eq. (4.2.1) generates $3! = 6$ fully contracted terms. Each term is made up of the product of 3 time ordered products of one creation and one destruction operator. Four out of six terms are given in Eq. (4.2.2)

(connected terms); the remaining two (disconnected) terms are given in Eq. (4.2.5). The linked cluster theorem[13] allows us to disregard the disconnected terms so that Eq. (4.2.1) gives

$$\begin{aligned}
&\langle T[a^+_{\boldsymbol{q}_1}(\tau_1)a^+_{\boldsymbol{q}_2}(\tau_1)a_{\boldsymbol{q}_3}(\tau_1)a_{\boldsymbol{q}_4}(\tau_1)a_{\boldsymbol{k}}(\tau)a^+_{\boldsymbol{k}}]\rangle_{\rm c}\\
&\quad=\langle T[a^+_{\boldsymbol{q}_1}(\tau_1)a_{\boldsymbol{k}}(\tau)]\rangle\langle T[a^+_{\boldsymbol{q}_2}(\tau_1)a_{\boldsymbol{q}_3}(\tau_1)]\rangle\langle T[a_{\boldsymbol{q}_4}(\tau_1)a^+_{\boldsymbol{k}}]\rangle\\
&\qquad+\langle T[a^+_{\boldsymbol{q}_1}(\tau_1)a_{\boldsymbol{k}}(\tau)]\rangle\langle T[a^+_{\boldsymbol{q}_2}(\tau_1)a_{\boldsymbol{q}_4}(\tau_1)]\rangle\langle T[a_{\boldsymbol{q}_3}(\tau_1)a^+_{\boldsymbol{k}}]\rangle\\
&\qquad+\langle T[a^+_{\boldsymbol{q}_1}(\tau_1)a_{\boldsymbol{q}_3}(\tau_1)]\rangle\langle T[a^+_{\boldsymbol{q}_2}(\tau_1)a_{\boldsymbol{k}}(\tau)]\rangle\langle T[a_{\boldsymbol{q}_4}(\tau_1)a^+_{\boldsymbol{k}}]\rangle\\
&\qquad+\langle T[a^+_{\boldsymbol{q}_1}(\tau_1)a_{\boldsymbol{q}_4}(\tau_1)]\rangle\langle T[a^+_{\boldsymbol{q}_2}(\tau_1)a_{\boldsymbol{k}}(\tau)]\rangle\langle T[a_{\boldsymbol{q}_3}(\tau_1)a^+_{\boldsymbol{k}}]\rangle. \qquad (4.2.2)
\end{aligned}$$

Using Eq. (4.1.20), we replace the time ordered products in Eq. (4.2.2) by the zero-order temperature Green function. For instance,

$$\langle T[a^+_{\boldsymbol{q}_1}(\tau_1)a_{\boldsymbol{k}}(\tau)]\rangle=-\delta_{\boldsymbol{q}_1,\boldsymbol{k}}\mathcal{G}^{(0)}_{\boldsymbol{k}}(\tau-\tau_1). \qquad (4.2.3a)$$

The time difference appearing in the argument of the unperturbed termperature Green function is given by the time argument of the destruction operator (the time at which the boson is destroyed) minus the time argument of the creation operator (the time at which the boson was created). A problem arises when both the destruction and creation operators have the *same* time argument. This occurs when both operators belong to the same interaction Hamiltonian, for instance the Hamiltonian $\mathcal{H}_{\rm int}(\tau_1)$ in Eq. (4.2.1). Since the creation operator always appears on the left of the destruction operator in the interaction Hamiltonian [see Eq. (4.1.5)], the time ordering operator must operate in such a way to assure this ordering. In particular, one has to assume that if the time of the destruction operator is τ_1, the time of the creation operator belonging to the same interaction Hamiltonian has to be chosen as $\tau_1+\eta$ where η is an infinitesimal *positive* time. For instance, the equal time ordered product occurring in the first term of the right-hand side of Eq. (4.2.2) has to be intended as

$$\lim_{\eta\to0^+}\langle T[a^+_{\boldsymbol{q}_2}(\tau_1+\eta)a_{\boldsymbol{q}_3}(\tau_1)]\rangle=-\delta_{\boldsymbol{q}_2,\boldsymbol{q}_3}\mathcal{G}^{(0)}_{\boldsymbol{q}_2}(0^-) \qquad (4.2.3b)$$

where 0^- is an infinitesimal *negative* time. By means of Eqs. (4.2.2), (4.2.3a), (4.2.3b) and from the invariance of the interaction potential (4.1.6b) under the permutation of the first two or the last two labels, Eq. (4.2.1) becomes

$$\mathcal{G}^{(1)}_{\boldsymbol{k}}(\tau)=-\frac{4}{\hbar}\sum_{\boldsymbol{p}}V_{\boldsymbol{k},\boldsymbol{p},\boldsymbol{k},\boldsymbol{p}}\int_0^{\beta\hbar}d\tau_1\mathcal{G}^{(0)}_{\boldsymbol{k}}(\tau-\tau_1)\mathcal{G}^{(0)}_{\boldsymbol{p}}(0^-)\mathcal{G}^{(0)}_{\boldsymbol{k}}(\tau_1). \qquad (4.2.4)$$

It is convenient to represent the right-hand side of Eq. (4.2.4) by a Feynman diagram as shown in Fig.4.1(a). Indeed, we have represented the potential interaction $V_{\boldsymbol{k},\boldsymbol{p},\boldsymbol{k},\boldsymbol{p}}$ by a small full circle with two outgoing lines representing unperturbed temperature Green functions with momenta given by the first two labels of the interaction potential and two incoming lines representing unperturbed temperature Green functions with momenta given by the last two labels of the interaction potential. The invariance of the interaction potential leads to a multiplicity factor of 4. In Fig. 4.1(a),

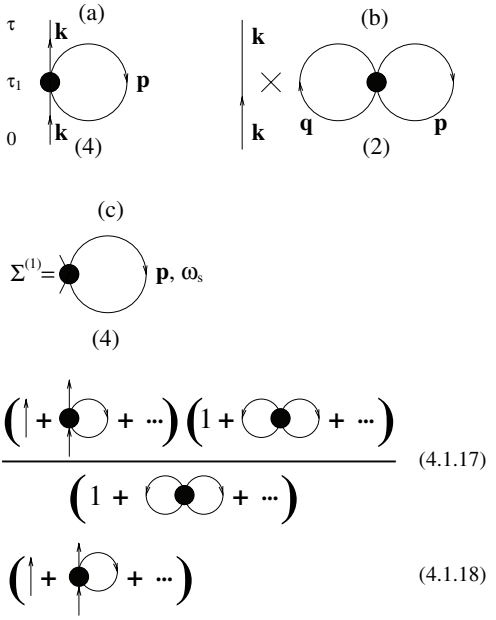

Fig. 4.1. First-order (a) connected and (b) disconnected Feynman diagrams and (c) first-order self-enrgy. The numbers in brackets below the diagrams give the multiplicity of the diagram. The lower part of the figure shows the first-order diagrammatic representation of Eqs. (4.1.17) and (4.1.18), respectively.

the lines going upwards (↑) and downwards (↓) are often called "particle"and "hole" lines, respectively. Note that the lines outoing from and entering the same interaction potential are *always* hole lines due to the choice (4.2.3b). The diagram shown in Fig. 4.1(a) is the only first-order "connected" diagram corresponding to Eq. (4.2.4) while the diagram shown in Fig. 4.1(b) is the only first-order "disconnected diagram" occurring in the numerator of Eq. (4.1.17) but not in Eq. (4.1.18). Indeed, the two disconnected terms occurring in the first-order expansion of the numerator of Eq. (4.1.17) are given by

$$\begin{aligned}&\langle T[a^+_{\boldsymbol{q}_1}(\tau_1)a_{\boldsymbol{q}_3}(\tau_1)]\rangle\langle T[a^+_{\boldsymbol{q}_2}(\tau_1)a_{\boldsymbol{q}_4}(\tau_1)]\rangle\langle T[a_{\boldsymbol{k}}(\tau)a^+_{\boldsymbol{k}}]\rangle\\ &\quad+\langle T[a^+_{\boldsymbol{q}_1}(\tau_1)a_{\boldsymbol{q}_4}(\tau_1)]\rangle\langle T[a^+_{\boldsymbol{q}_2}(\tau_1)a_{\boldsymbol{q}_3}(\tau_1)]\rangle\langle T[a_{\boldsymbol{k}}(\tau)a^+_{\boldsymbol{k}}]\rangle,\end{aligned}\tag{4.2.5}$$

leading to the contribution

$$-\frac{2}{\hbar}\sum_{\boldsymbol{p},\boldsymbol{q}}V_{\boldsymbol{q}_1,\boldsymbol{q}_2,\boldsymbol{q}_1,\boldsymbol{q}_2}\;\beta\hbar\mathcal{G}^{(0)}_{\boldsymbol{k}}(\tau)\mathcal{G}^{(0)}_{\boldsymbol{q}_1}(0^-)\mathcal{G}^{(0)}_{\boldsymbol{q}_2}(0^-).\tag{4.2.6}$$

The same contribution without $\mathcal{G}^{(0)}_{\boldsymbol{k}}(\tau)$ comes from the first-order term of the denominator of Eq. (4.1.17). The first terms of the series expansion of the numerator and denominator of Eq. (4.1.17) are shown in the lower part of Fig. 4.1. One can infer the great importance of the linked cluster theorem by comparing the diagrammatic expansion of Eq. (4.1.17) and (4.1.18) in Fig. 4.1.

The Fourier series of the first-order temperature Green function can be obtained from Eq. (4.2.4) using Eq. (4.1.22) for the unperturbed temperature Green functions. One has

$$\mathcal{G}_{\boldsymbol{k}}^{(1)}(\tau) = -\frac{4}{\hbar}\sum_{\boldsymbol{p}} V_{\boldsymbol{k},\boldsymbol{p},\boldsymbol{k},\boldsymbol{p}} \left(\frac{1}{\beta\hbar}\right)^3 \sum_{n,s,m} \mathcal{G}_{\boldsymbol{k}}^{(0)}(i\omega_n)\mathcal{G}_{\boldsymbol{p}}^{(0)}(i\omega_s)\mathcal{G}_{\boldsymbol{k}}^{(0)}(i\omega_m)$$
$$\times e^{-i\omega_n\tau} e^{i\omega_s\eta} \int_0^{\beta\hbar} d\tau_1 e^{-i(\omega_m-\omega_n)\tau_1} \tag{4.2.7}$$

where η is the infinitesimal positive quantity defined in Eq. (4.2.3b). By means of Eq. (4.1.23), the time integral in Eq. (4.2.7) gives

$$\int_0^{\beta\hbar} d\tau_1 e^{i(\omega_n-\omega_m)\tau_1} = \beta\hbar\delta_{m,n} \tag{4.2.8}$$

and Eq. (4.2.7) becomes

$$\mathcal{G}_{\boldsymbol{k}}^{(1)}(\tau) = \frac{1}{\beta\hbar}\sum_n e^{-i\omega_n\tau}[\mathcal{G}_{\boldsymbol{k}}^{(0)}(i\omega_n)]^2\Sigma^{(1)}(\boldsymbol{k}) \tag{4.2.9}$$

where the first-order self-energy is given by

$$\Sigma^{(1)}(\boldsymbol{k}) = -\frac{4}{\hbar}\sum_{\boldsymbol{p}} V_{\boldsymbol{k},\boldsymbol{p},\boldsymbol{k},\boldsymbol{p}} \frac{1}{\beta\hbar}\sum_s \frac{e^{i\omega_s\eta}}{i\omega_s - \omega_{\boldsymbol{p}}}. \tag{4.2.10}$$

Comparing Eq. (4.2.9) with Eq. (4.1.22), one has

$$\mathcal{G}_{\boldsymbol{k}}^{(1)}(i\omega_n) = [\mathcal{G}_{\boldsymbol{k}}^{(0)}(i\omega_n)]^2\Sigma^{(1)}(\boldsymbol{k}). \tag{4.2.11}$$

The diagram corresponding to the first-order self-energy (4.2.10) is shown in Fig. 4.1(c). Let us give some general rules that make it possible to pass from Fyenman diagrams to analytic forms and vice versa:

i) Associate a full circle with two outgoing and two incoming lines to each interaction potential. In Figs. 4.1(a) and (c), the *multiplicity* factor 4 is due to the number of equivalent diagrams that can be obtained after exchanging the outgoing lines (2) and the incoming lines (2).

ii) Associate an unperturbed temperature Green function $\mathcal{G}_{\boldsymbol{p}}^{(0)}(\tau - \tau')$ (time diagrams) or

$$\mathcal{G}_{\boldsymbol{p}}^{(0)}(i\omega_s) = \frac{1}{i\omega_s - \omega_{\boldsymbol{p}}} \tag{4.2.12}$$

in the self-energy (frequency) diagrams to each line of the diagram. If the unperturbed temperature Green function makes a closed loop, the time argument is $\tau = 0^-$ and a factor $e^{i\omega_s\eta}$ with $\eta \to 0^+$ has to be associated to the frequency Green function (4.2.12), in agreement with Eqs. (4.2.3b) and (4.1.22). Note that

the two short "external" lines in the diagram (c) of Fig. 4.1 are reminiscent of the term $[\mathcal{G}^{(0)}_{\boldsymbol{k}}(i\omega_n)]^2$ of Eq. (4.2.11).

iii) The δ-function occurring in the interaction potential (4.1.6a) implies the momentum conservation at each interaction: the sum of the momenta of the outgoing lines must be equal to the sum of the momenta of the incoming lines.

iv) Equation (4.2.8) implies the "frequency" conservation at each interaction. Note that the arrows that in the time space correspond to "particle" or "hole" lines, in the frequency space (self-energy diagrams) they correspond to a sort of "current" that has to be conserved at each "node".

v) A sum over the "internal" momenta in the time diagrams and a sum over both the internal momenta and frequencies times a factor $\frac{1}{\beta\hbar}$ for the self-energy diagrams have to be performed. Obviously, no sum has to be performed over the "external" momentum $\boldsymbol{k}$ and the external frequency ω_n. In the self-energy diagram of Fig. 4.1(c), a sum over $\boldsymbol{p}$ and $\omega_s = \frac{2\pi s}{\beta\hbar}$ (or simply a sum over s) has to be carried out.

vi) A factor $(-1/\hbar)^n$ has to be added where n is the order of the perturbation.

Using the rules i)–vi), the translation of Eq. (4.2.10) into the diagram of Fig. 4.1(c) and vice versa is direct. Let us now evaluate explicitly the frequency sum occurring in Eq. (4.2.10). To do this,[13] we introduce the meromorphic function on the complex plane z

$$f_1(z) = \frac{e^{\eta z}}{e^{\beta\hbar z} - 1} \; \frac{1}{z - \omega_{\boldsymbol{p}}}. \tag{4.2.13}$$

A meromorphic[35] function is analytic everywhere in the complex plane except at a discrete number of poles. As one can see, the function $f_1(z)$ defined in Eq. (4.2.13) has isolated simple poles on the imaginary axis at the points $z = i\omega_s = i\frac{2\pi s}{\beta\hbar}$ where s is an integer and on the real axis at $z = \omega_{\boldsymbol{p}}$. Moreover, the function $f_1(z)$ vanishes on the circle Γ of radius $|z| \to \infty$. Indeed, for $\Re z > 0$, one has $f_1(z) \to \frac{1}{z} e^{-\beta\hbar z}$ and for $\Re z < 0$, one has $f_1(z) \to -\frac{1}{z} e^{\eta z}$. If we integrate the function $f_1(z)$ along the circle Γ and take the limit $|z| \to \infty$, we obtain

$$\lim_{|z|\to\infty} \oint_\Gamma f_1(z) dz = 0 \tag{4.2.14}$$

since the function $f_1(z)$ goes to zero faster than $1/z$ for $|z| \to \infty$. On the other hand, if we apply the residue theorem[35] to the meromorphic function $f_1(z)$ along the contour Γ, we obtain

$$\oint_\Gamma f_1(z) dz = 2\pi i \left(\frac{1}{\beta\hbar} \sum_s \frac{e^{i\omega_s \eta}}{i\omega_s - \omega_{\boldsymbol{p}}} + \frac{e^{\eta\omega_p}}{e^{\beta\hbar\omega_p} - 1} \right) \tag{4.2.15}$$

since inside the contour Γ, the function $f_1(z)$ has simple poles on the imaginary axis at $z = i\omega_s$ each with residue

$$\frac{1}{\beta\hbar} \; \frac{e^{i\omega_s \eta}}{i\omega_s - \omega_{\boldsymbol{p}}}$$

and on the real axis at $z = \omega_{\boldsymbol{p}}$ with residue

$$\frac{e^{\eta\omega_p}}{e^{\beta\hbar\omega_p} - 1}.$$

In the limit $\eta \to 0$, Eqs. (4.2.14) and (4.2.15) lead to the relationship

$$\lim_{\eta\to 0} \frac{1}{\beta\hbar} \sum_s \frac{e^{i\omega_s\eta}}{i\omega_s - \omega_{\boldsymbol{p}}} = -n_{\boldsymbol{p}}^{(0)}. \tag{4.2.16}$$

Using Eqs. (4.2.16), (4.1.6a) and (4.1.6b), the first-order self-energy (4.2.10) becomes

$$\Sigma^{(1)}(\boldsymbol{k}) = \frac{4}{\hbar} \sum_{\boldsymbol{p}} V_{\boldsymbol{k},\boldsymbol{p},\boldsymbol{k},\boldsymbol{p}} n_{\boldsymbol{p}}^{(0)} = -\alpha \frac{\omega_{\boldsymbol{k}}}{S} \tag{4.2.17}$$

where α is given by Eq. (3.6.3). Equation (4.2.17) coincides with the first-order self-energy (3.6.2) obtained by means of the method of the Green function equation of motion.

4.3. Second-Order Perturbation Theory

The second-order temperature Green function, given by the term with $n = 2$ of Eq. (4.1.18), reads

$$\begin{aligned}
\mathcal{G}_{\boldsymbol{k}}^{(2)}(\tau) &= -\frac{1}{2!\ \hbar^2} \int_0^{\beta\hbar} d\tau_1 \int_0^{\beta\hbar} d\tau_2 \langle T[\mathcal{H}_{\rm int}(\tau_1)\mathcal{H}_{\rm int}(\tau_2) a_{\boldsymbol{k}}(\tau) a_{\boldsymbol{k}}^+] \rangle_{\rm c} \\
&= -\frac{1}{2!\ \hbar^2} \sum_{\boldsymbol{q}_1,\boldsymbol{q}_2,\boldsymbol{q}_3,\boldsymbol{q}_4} V_{\boldsymbol{q}_1,\boldsymbol{q}_2,\boldsymbol{q}_3,\boldsymbol{q}_4} \sum_{\boldsymbol{q}_5,\boldsymbol{q}_6,\boldsymbol{q}_7,\boldsymbol{q}_8} V_{\boldsymbol{q}_5,\boldsymbol{q}_6,\boldsymbol{q}_7,\boldsymbol{q}_8} \int_0^{\beta\hbar} d\tau_1 \int_0^{\beta\hbar} d\tau_2 \\
&\quad \times \langle T[a_{\boldsymbol{q}_1}^+(\tau_1) a_{\boldsymbol{q}_2}^+(\tau_1) a_{\boldsymbol{q}_3}(\tau_1) a_{\boldsymbol{q}_4}(\tau_1) a_{\boldsymbol{q}_5}^+(\tau_2) \\
&\quad \times a_{\boldsymbol{q}_6}^+(\tau_2) a_{\boldsymbol{q}_7}(\tau_2) a_{\boldsymbol{q}_8}(\tau_2) a_{\boldsymbol{k}}(\tau) a_{\boldsymbol{k}}^+] \rangle_{\rm c}.
\end{aligned} \tag{4.3.1}$$

The generalized Wick's theorem applied to Eq. (4.3.1) generates $5! = 120$ fully contracted terms: 80 terms lead to connected diagrams, 40 to disconnected diagrams. The invariance property of the interaction potential allows us to group the connected diagrams into 6 distinct terms:

$$\begin{aligned}
\mathcal{G}_{\boldsymbol{k}}^{(2)}(\tau) = \frac{16}{2!\ \hbar^2} \sum_{\boldsymbol{p},\boldsymbol{q}} V_{\boldsymbol{k},\boldsymbol{p},\boldsymbol{k},\boldsymbol{p}} V_{\boldsymbol{k},\boldsymbol{q},\boldsymbol{k},\boldsymbol{q}} \int_0^{\beta\hbar} d\tau_1 \int_0^{\beta\hbar} d\tau_2 \big[\mathcal{G}_{\boldsymbol{k}}^{(0)}(\tau - \tau_2) \\
\times \mathcal{G}_{\boldsymbol{p}}^{(0)}(0^-) \mathcal{G}_{\boldsymbol{k}}^{(0)}(\tau_2 - \tau_1) \mathcal{G}_{\boldsymbol{q}}^{(0)}(0^-) \mathcal{G}_{\boldsymbol{k}}^{(0)}(\tau_1) + \mathcal{G}_{\boldsymbol{k}}^{(0)}(\tau - \tau_1) \\
\times \mathcal{G}_{\boldsymbol{p}}^{(0)}(0^-) \mathcal{G}_{\boldsymbol{k}}^{(0)}(\tau_1 - \tau_2) \mathcal{G}_{\boldsymbol{q}}^{(0)}(0^-) \mathcal{G}_{\boldsymbol{k}}^{(0)}(\tau_2) \big] \\
+ \frac{16}{2!\ \hbar^2} \sum_{\boldsymbol{p},\boldsymbol{q}} V_{\boldsymbol{k},\boldsymbol{q},\boldsymbol{k},\boldsymbol{q}} V_{\boldsymbol{q},\boldsymbol{p},\boldsymbol{q},\boldsymbol{p}} \int_0^{\beta\hbar} d\tau_1 \int_0^{\beta\hbar} d\tau_2 \big[\mathcal{G}_{\boldsymbol{k}}^{(0)}(\tau - \tau_2)
\end{aligned}$$

$$\times \mathcal{G}_{\boldsymbol{q}}^{(0)}(\tau_2-\tau_1)\mathcal{G}_{\boldsymbol{q}}^{(0)}(\tau_1-\tau_2)\mathcal{G}_{\boldsymbol{p}}^{(0)}(0^-)\mathcal{G}_{\boldsymbol{k}}^{(0)}(\tau_2)+\mathcal{G}_{\boldsymbol{k}}^{(0)}(\tau-\tau_1)$$

$$\times \mathcal{G}_{\boldsymbol{q}}^{(0)}(\tau_1-\tau_2)\mathcal{G}_{\boldsymbol{q}}^{(0)}(\tau_2-\tau_1)\mathcal{G}_{\boldsymbol{p}}^{(0)}(0^-)\mathcal{G}_{\boldsymbol{k}}^{(0)}(\tau_1)\big]$$

$$+\frac{8}{2!\,\hbar^2}\sum_{\boldsymbol{q}_1,\boldsymbol{q}_2,\boldsymbol{p}} V_{\boldsymbol{k},\boldsymbol{p},\boldsymbol{q}_1,\boldsymbol{q}_2}V_{\boldsymbol{q}_1,\boldsymbol{q}_2,\boldsymbol{k},\boldsymbol{p}}\int_0^{\beta\hbar}d\tau_1\int_0^{\beta\hbar}d\tau_2\big[\mathcal{G}_{\boldsymbol{k}}^{(0)}(\tau-\tau_2)$$

$$\times \mathcal{G}_{\boldsymbol{q}_1}^{(0)}(\tau_2-\tau_1)\mathcal{G}_{\boldsymbol{q}_2}^{(0)}(\tau_2-\tau_1)\mathcal{G}_{\boldsymbol{p}}^{(0)}(\tau_1-\tau_2)\mathcal{G}_{\boldsymbol{k}}^{(0)}(\tau_1)+G_{\boldsymbol{k}}^{(0)}(\tau-\tau_1)$$

$$\times \mathcal{G}_{\boldsymbol{q}_1}^{(0)}(\tau_1-\tau_2)\mathcal{G}_{\boldsymbol{q}_2}^{(0)}(\tau_1-\tau_2)\mathcal{G}_{\boldsymbol{p}}^{(0)}(\tau_2-\tau_1)\mathcal{G}_{\boldsymbol{k}}^{(0)}(\tau_2)\big]. \qquad (4.3.2)$$

The first and second term in the right-hand side of Eq. (4.3.2) can be identified with the Feynman diagrams (a_1) and (a_2) of Fig. 4.2, respectively; the third and fourth term with the diagrams (b_1) and (b_2); the fifth and sixth term with diagrams (c_1) and (c_2). Note that the second, fourth and sixth integral of Eq. (4.3.2) reduce to the first, third and fifth integral, respectively, by the change of the integration variables. From a topological point of view, this means that the diagrams (a_2), (b_2) and (c_2)

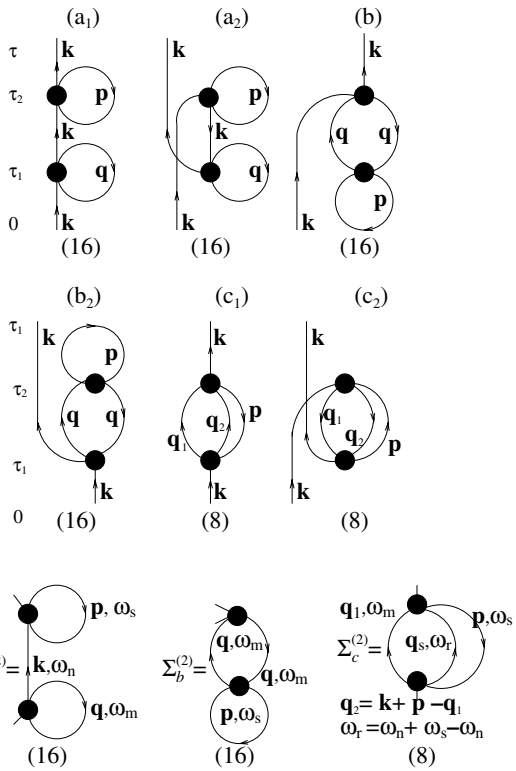

Fig. 4.2. Second-order connected Feynman diagrams (time space) (a_1), (a_2), (b_1), (b_2), (c_1), (c_2) and second-order self-energies (frequency space) $\Sigma_a^{(2)}$, $\Sigma_b^{(2)}$, $\Sigma_c^{(2)}$. The numbers whitin the brackets under the diagrams give their multiplicity. The couples of time diagrams (a_1) and (a_2), (b_1) and (b_2), (c_1) and (c_2) are topologically equivalent.

reduce to (a_1), (b_1) and (c_1), respectively, pulling both ends of the external lines. Such a symmetry suggests a more general rule:

vii) Each of the $n!$ permutations of the time variables τ_1, $\tau_2, \cdots, \tau_n$ in the n-th term of series in Eq. (4.1.18) leads to the same contribution such that the corresponding diagrams are defined as "topologically equivalent". Then, we may suppress the factor $\frac{1}{n!}$ in the n-th term of the series expansion, keeping only *topologically distinct* diagrams.

For example, in Fig. 4.2, associating a multiplicity $16 \times 2!$ to diagrams (a_1) and (b_1) and a multiplicity $8 \times 2!$ to diagram (c_1), these only three diagrams represent the 80 connected terms coming from the second-order perturbation expansion of Eq. (4.3.1). Using Eq. (4.1.22), the second-order temperature Green function (4.3.2) becomes

$$\begin{aligned}
\mathcal{G}^{(2)}_{\boldsymbol{k}}(\tau) = \frac{16}{\hbar^2}\sum_{\boldsymbol{p},\boldsymbol{q}} V_{\boldsymbol{k},\boldsymbol{p},\boldsymbol{k},\boldsymbol{p}} V_{\boldsymbol{k},\boldsymbol{q},\boldsymbol{k},\boldsymbol{q}} \left(\frac{1}{\beta\hbar}\right)^5 \sum_{n,r,s,t,m} \mathcal{G}^{(0)}_{\boldsymbol{k}}(i\omega_n)\mathcal{G}^{(0)}_{\boldsymbol{p}}(i\omega_s)\mathcal{G}^{(0)}_{\boldsymbol{k}}(i\omega_t) \\
\times \mathcal{G}^{(0)}_{\boldsymbol{q}}(i\omega_r)\mathcal{G}^{(0)}_{\boldsymbol{k}}(i\omega_m) e^{-i\omega_n\tau} e^{i\omega_s\eta} e^{i\omega_r\eta} \int_0^{\beta\hbar} d\tau_1 \; e^{-i(\omega_m-\omega_t)\tau_1} \\
\times \int_0^{\beta\hbar} d\tau_2 \; e^{-i(\omega_t-\omega_m)\tau_2} + \frac{16}{\hbar^2}\sum_{\boldsymbol{p},\boldsymbol{q}} V_{\boldsymbol{k},\boldsymbol{q},\boldsymbol{k},\boldsymbol{q}} V_{\boldsymbol{q},\boldsymbol{p},\boldsymbol{q},\boldsymbol{p}} \left(\frac{1}{\beta\hbar}\right)^5 \\
\sum_{n,r,s,t,m} \mathcal{G}^{(0)}_{\boldsymbol{k}}(i\omega_n)\mathcal{G}^{(0)}_{\boldsymbol{q}}(i\omega_r)\mathcal{G}^{(0)}_{\boldsymbol{q}}(i\omega_t)\mathcal{G}^{(0)}_{\boldsymbol{p}}(i\omega_s)\mathcal{G}^{(0)}_{\boldsymbol{k}}(i\omega_m) e^{-i\omega_n\tau} e^{i\omega_s\eta} \\
\times \int_0^{\beta\hbar} d\tau_1 e^{-i(\omega_t-\omega_r)\tau_1} \int_0^{\beta\hbar} d\tau_2 e^{-i(\omega_r-\omega_m-\omega_t+\omega_m)\tau_2} \\
+ \frac{8}{\hbar^2}\sum_{\boldsymbol{q}_1,\boldsymbol{q}_2,\boldsymbol{p}} V_{\boldsymbol{k},\boldsymbol{p},\boldsymbol{q}_1,\boldsymbol{q}_2} V_{\boldsymbol{q}_1,\boldsymbol{q}_2,\boldsymbol{k},\boldsymbol{p}} \left(\frac{1}{\beta\hbar}\right)^5 \sum_{n,r,s,t,m} \mathcal{G}^{(0)}_{\boldsymbol{k}}(i\omega_n) \\
\times \mathcal{G}^{(0)}_{\boldsymbol{q}_1}(i\omega_r)\mathcal{G}^{(0)}_{\boldsymbol{q}_2}(i\omega_t)\mathcal{G}^{(0)}_{\boldsymbol{p}}(i\omega_s)\mathcal{G}^{(0)}_{\boldsymbol{k}}(i\omega_m) e^{-i\omega_n\tau} \\
\times \int_0^{\beta\hbar} d\tau_1 \; e^{-i(\omega_r+\omega_t-\omega_s-\omega_m)\tau_1} \int_0^{\beta\hbar} d\tau_2 e^{-i(\omega_r-\omega_n+\omega_t-\omega_s)\tau_2}. \qquad (4.3.3)
\end{aligned}$$

The integrals over τ_1 and τ_2 can be evaluated by means of Eq. (4.2.8): each integral gives a δ-function that accounts for the frequency conservation as established in the iv) rule of Section 4.2. By means of Eq. (4.1.22), the second-order frequency Green function becomes

$$\mathcal{G}^{(2)}_{\boldsymbol{k}}(i\omega_n) = [\mathcal{G}^{(0)}_{\boldsymbol{k}}(i\omega_n)]^2[\Sigma^{(2)}_a(\boldsymbol{k}, i\omega_n) + \Sigma^{(2)}_b(\boldsymbol{k}) + \Sigma^{(2)}_c(\boldsymbol{k}, i\omega_n)] \qquad (4.3.4)$$

where $\Sigma^{(2)}_a$, $\Sigma^{(2)}_b$ and $\Sigma^{(2)}_c$ are the second-order self-energies shown in Fig. 4.2. The analytic form of such self-energies can be obtained directly from Eq. (4.3.3) or using

the rules i)–vi) of Section 4.2. Indeed, the self-enegy $\Sigma_a^{(2)}$ is given by

$$\Sigma_a^{(2)}(\boldsymbol{k}, i\omega_n) = \mathcal{G}_{\boldsymbol{k}}^{(0)}(i\omega_n)\frac{16}{\hbar^2}\sum_{\boldsymbol{p},\boldsymbol{q}} V_{\boldsymbol{k},\boldsymbol{p},\boldsymbol{k},\boldsymbol{p}} V_{\boldsymbol{k},\boldsymbol{q},\boldsymbol{k},\boldsymbol{q}}\ \frac{1}{\beta\hbar}\sum_s \frac{e^{i\omega_s\eta}}{i\omega_s - \omega_{\boldsymbol{p}}}$$

$$\times \frac{1}{\beta\hbar}\sum_m \frac{e^{i\omega_m\eta}}{i\omega_m - \omega_{\boldsymbol{q}}} = \mathcal{G}_{\boldsymbol{k}}^{(0)}(i\omega_n)\left[\Sigma^{(1)}(\boldsymbol{k})\right]^2 \tag{4.3.5}$$

where the first-order self-energy $\Sigma^{(1)}$ is given by Eq. (4.2.10) or (4.2.17). The self-energy $\Sigma_b^{(2)}$ is given by

$$\Sigma_b^{(2)}(\boldsymbol{k}) = \frac{16}{\hbar^2}\sum_{\boldsymbol{p},\boldsymbol{q}} V_{\boldsymbol{k},\boldsymbol{q},\boldsymbol{k},\boldsymbol{q}} V_{\boldsymbol{q},\boldsymbol{p},\boldsymbol{q},\boldsymbol{p}}\ \frac{1}{\beta\hbar}\sum_m \frac{1}{(i\omega_m - \omega_{\boldsymbol{q}})^2}\frac{1}{\beta\hbar}\sum_s \frac{e^{i\omega_s\eta}}{i\omega_s - \omega_{\boldsymbol{p}}}$$

$$= -4\beta\sum_{\boldsymbol{q}} V_{\boldsymbol{k},\boldsymbol{q},\boldsymbol{k},\boldsymbol{q}}\ n_{\boldsymbol{q}}^{(0)}(1 + n_{\boldsymbol{q}}^{(0)})\ \Sigma^{(1)}(\boldsymbol{q}) \tag{4.3.6}$$

where $\Sigma^{(1)}$ is given by Eq. (4.2.10) and the relationship

$$\frac{1}{\beta\hbar}\sum_m \frac{1}{(i\omega_m - \omega_{\boldsymbol{q}})^2} = \beta\hbar\ n_{\boldsymbol{q}}^{(0)}(1 + n_{\boldsymbol{q}}^{(0)}) \tag{4.3.7}$$

has been used. To prove Eq. (4.3.7), we introduce the meromorphic function

$$f_2(z) = \frac{1}{e^{\beta\hbar z} - 1}\ \frac{1}{(z - \omega_{\boldsymbol{q}})^2} \tag{4.3.8}$$

which has a discrete set of simple poles along the imaginary axis located at $z = i\omega_m = \frac{2i\pi r}{\beta\hbar}$ with residue

$$\frac{1}{\beta\hbar}\ \frac{1}{(i\omega_m - \omega_{\boldsymbol{q}})^2}$$

and a pole of order two on the real axis at $z = \omega_{\boldsymbol{q}}$ with residue

$$-\beta\hbar\frac{e^{\beta\hbar\omega_q}}{\left(e^{\beta\hbar\omega_q} - 1\right)^2} = -\beta\hbar\ n_{\boldsymbol{q}}^{(0)}(1 + n_{\boldsymbol{q}}^{(0)}).$$

Then the residue theorem applied to the function $f_2(z)$ around the the circle Γ with radius $|z| \to \infty$ gives

$$\oint_\Gamma f_2(z)dz = 2\pi i\left[\frac{1}{\beta\hbar}\sum_m \frac{1}{(i\omega_m - \omega_{\boldsymbol{q}})^2} - \beta\hbar\ n_{\boldsymbol{q}}^{(0)}(1 + n_{\boldsymbol{q}}^{(0)})\right]. \tag{4.3.9}$$

Since the function $f_2(z)$ on the circle Γ goes to zero at least as $\frac{1}{z^2}$ for $|z| \to \infty$, the integral on the left-hand side of Eq. (4.3.9) vanishes and Eq. (4.3.7) is proven. The

self-energy $\Sigma_c^{(2)}$ is given by

$$\Sigma_c^{(2)}(\boldsymbol{k}, i\omega_n) = \frac{8}{\hbar^2} \sum_{\boldsymbol{q}_1,\boldsymbol{q}_2,\boldsymbol{p}} V_{\boldsymbol{k},\boldsymbol{p},\boldsymbol{q}_1,\boldsymbol{q}_2} V_{\boldsymbol{q}_1,\boldsymbol{q}_2,\boldsymbol{k},\boldsymbol{p}} \frac{1}{\beta\hbar} \sum_s \frac{1}{i\omega_s - \omega_{\boldsymbol{p}}} \times \frac{1}{\beta\hbar} \sum_m \frac{1}{i\omega_m - \omega_{\boldsymbol{q}_1}} \frac{1}{i\omega_n + i\omega_s - i\omega_m - \omega_{\boldsymbol{q}_2}}. \quad (4.3.10)$$

The sum over m in Eq. (4.3.10) can be evaluated as follows

$$\begin{aligned} &\frac{1}{\beta\hbar} \sum_m \frac{1}{i\omega_m - \omega_{\boldsymbol{q}_1}} \frac{1}{i\omega_n + i\omega_s - i\omega_m - \omega_{\boldsymbol{q}_2}} \\ &= \frac{1}{i\omega_n + i\omega_s - \omega_{\boldsymbol{q}_1} - \omega_{\boldsymbol{q}_2}} \frac{1}{\beta\hbar} \sum_m \left(\frac{1}{i\omega_m - \omega_{\boldsymbol{q}_1}} - \frac{1}{i\omega_m - i\omega_n - i\omega_s + \omega_{\boldsymbol{q}_2}} \right) \\ &= \frac{-n^{(0)}_{\boldsymbol{q}_1} + n(i\omega_n + i\omega_s - \omega_{\boldsymbol{q}_2})}{i\omega_n + i\omega_s - \omega_{\boldsymbol{q}_1} - \omega_{\boldsymbol{q}_2}} = -\frac{1 + n^{(0)}_{\boldsymbol{q}_1} + n^{(0)}_{\boldsymbol{q}_2}}{i\omega_n + i\omega_s - \omega_{\boldsymbol{q}_1} - \omega_{\boldsymbol{q}_2}} \end{aligned} \quad (4.3.11)$$

where the last step is obtained using Eqs. (4.2.16) and (4.1.23) that gives

$$n(i\omega_n + i\omega_s - \omega_{\boldsymbol{q}_2}) = n(-\omega_{\boldsymbol{q}_2}) = -(1 + n^{(0)}_{\boldsymbol{q}_2}). \quad (4.3.12)$$

Replacing Eq. (4.3.11) into Eq. (4.3.10), one obtains

$$\Sigma_c^{(2)}(\boldsymbol{k}, i\omega_n) = -\frac{8}{\hbar^2} \sum_{\boldsymbol{q}_1,\boldsymbol{q}_2,\boldsymbol{p}} V_{\boldsymbol{k},\boldsymbol{p},\boldsymbol{q}_1,\boldsymbol{q}_2} V_{\boldsymbol{q}_1,\boldsymbol{q}_2,\boldsymbol{k},\boldsymbol{p}} (1 + n^{(0)}_{\boldsymbol{q}_1} + n^{(0)}_{\boldsymbol{q}_2}) \times \frac{1}{\beta\hbar} \sum_s \frac{1}{i\omega_s - \omega_{\boldsymbol{p}}} \frac{1}{i\omega_s + i\omega_n - \omega_{\boldsymbol{q}_1} - \omega_{\boldsymbol{q}_2}}. \quad (4.3.13)$$

The sum over s in Eq. (4.3.13) can be evaluated by repeating the same steps used in Eq. (4.3.11). One obtains

$$\begin{aligned} &\frac{1}{\beta\hbar} \sum_s \frac{1}{i\omega_s - \omega_{\boldsymbol{p}}} \frac{1}{i\omega_s + i\omega_n - \omega_{\boldsymbol{q}_1} - \omega_{\boldsymbol{q}_2}} \\ &= \frac{-n^{(0)}_{\boldsymbol{p}} + n(-i\omega_n + \omega_{\boldsymbol{q}_1} + \omega_{\boldsymbol{q}_2})}{i\omega_n - \omega_{\boldsymbol{q}_1} - \omega_{\boldsymbol{q}_2} + \omega_{\boldsymbol{p}}} \\ &= -\frac{1}{i\omega_n - \omega_{\boldsymbol{q}_1} - \omega_{\boldsymbol{q}_2} + \omega_{\boldsymbol{p}}} \frac{n^{(0)}_{\boldsymbol{p}}(1 + n^{(0)}_{\boldsymbol{q}_1} + n^{(0)}_{\boldsymbol{q}_2}) - n^{(0)}_{\boldsymbol{q}_1} n^{(0)}_{\boldsymbol{q}_2}}{1 + n^{(0)}_{\boldsymbol{q}_1} + n^{(0)}_{\boldsymbol{q}_2}} \end{aligned} \quad (4.3.14)$$

where the relationship

$$n(-i\omega_n + \omega_{\boldsymbol{q}_1} + \omega_{\boldsymbol{q}_2}) = n(\omega_{\boldsymbol{q}_1} + \omega_{\boldsymbol{q}_2}) = \frac{n^{(0)}_{\boldsymbol{q}_1} n^{(0)}_{\boldsymbol{q}_2}}{1 + n^{(0)}_{\boldsymbol{q}_1} + n^{(0)}_{\boldsymbol{q}_2}} \quad (4.3.15)$$

has been used. Replacing Eq. (4.3.14) into Eq. (4.3.13), one obtains

$$\Sigma_c^{(2)}(\boldsymbol{k}, i\omega_n) = \frac{8}{\hbar^2} \sum_{\boldsymbol{q}_1,\boldsymbol{q}_2,\boldsymbol{p}} V_{\boldsymbol{k},\boldsymbol{p},\boldsymbol{q}_1,\boldsymbol{q}_2} V_{\boldsymbol{q}_1,\boldsymbol{q}_2,\boldsymbol{k},\boldsymbol{p}} \frac{n_{\boldsymbol{p}}^{(0)}(1 + n_{\boldsymbol{q}_1}^{(0)} + n_{\boldsymbol{q}_2}^{(0)}) - n_{\boldsymbol{q}_1}^{(0)} n_{\boldsymbol{q}_2}^{(0)}}{i\omega_n - \omega_{\boldsymbol{q}_1} - \omega_{\boldsymbol{q}_2} + \omega_{\boldsymbol{p}}}. \tag{4.3.16}$$

By means of Eq. (4.1.6a), one can see that $\Sigma_a^{(2)}$ given by Eq. (4.3.5), $\Sigma_b^{(2)}$ given by Eq. (4.3.6) and $\Sigma_c^{(2)}$ given by Eq. (4.3.16) coincide with the corresponding second-order self-energies (3.4.21), (3.4.22) and (3.4.23) obtained by the method of the Green function equation of motion. This result supports the equivalence of the two perturbation approaches. The diagrams correspoding to $\Sigma_a^{(2)}$, $\Sigma_b^{(2)}$ and $\Sigma_c^{(2)}$ are shown in the lower part of Fig. 4.2. As explained in Section 3.5, the self-energy $\Sigma_a^{(2)}$ is "reducible" so that it does not appear in the denominator of Eq. (3.5.1). In the frame of the Feynman diagram expansion, a *reducible* self-energy diagram is a diagram that becomes disconnected "cutting" one line of the diagram so that the next general rule can be established:

viii) Only *irreducible* diagrams have to be retained in the *proper* self-energy $\Sigma^*(\boldsymbol{k}, i\omega_n)$. As one can see from Fig. 4.2, the diagram corresponding to the self-energy $\Sigma_a^{(2)}$ is *reducible* because it becomes disconnected cutting the line corresponding to $\mathcal{G}_{\boldsymbol{k}}^{(0)}(i\omega_n)$.

4.4. Third-order Perturbation Theory

As remarked in Section 4.3, both the diagram expansion and the method of the Green function equation of motion lead to the same second-order self-energy. However, to illustrate the power of the diagram expansion, we evaluate the third-order proper self-energy in this section, an almost hopeless attempt using the method of the equation of motion. The third-order self-energy, that never appears in literature, can be an useful exercise to become familiarised with the diagram technique in magnetism. The third-order temperature Green function is given by the term with $n = 3$ of the perturbation expansion (4.1.18) that is

$$\begin{aligned}
\mathcal{G}_{\boldsymbol{k}}^{(3)}(\tau) &= \frac{1}{3!\,\hbar^3} \int_0^{\beta\hbar} d\tau_1 \int_0^{\beta\hbar} d\tau_2 \int_0^{\beta\hbar} d\tau_3 \langle T[\mathcal{H}_{\rm int}(\tau_1)\mathcal{H}_{\rm int}(\tau_2)\mathcal{H}_{\rm int}(\tau_3) a_{\boldsymbol{k}}(\tau) a_{\boldsymbol{k}}^+] \rangle_{\rm c} \\
&= \frac{1}{3!\,\hbar^3} \sum_{\boldsymbol{q}_1,\boldsymbol{q}_2,\boldsymbol{q}_3,\boldsymbol{q}_4} V_{\boldsymbol{q}_1,\boldsymbol{q}_2,\boldsymbol{q}_3,\boldsymbol{q}_4} \sum_{\boldsymbol{q}_5,\boldsymbol{q}_6,\boldsymbol{q}_7,\boldsymbol{q}_8} V_{\boldsymbol{q}_5,\boldsymbol{q}_6,\boldsymbol{q}_7,\boldsymbol{q}_8} \\
&\quad \times \sum_{\boldsymbol{q}_9,\boldsymbol{q}_{10},\boldsymbol{q}_{11},\boldsymbol{q}_{12}} V_{\boldsymbol{q}_9,\boldsymbol{q}_{10},\boldsymbol{q}_{11},\boldsymbol{q}_{12}} \int_0^{\beta\hbar} d\tau_1 \int_0^{\beta\hbar} d\tau_2 \int_0^{\beta\hbar} d\tau_2 \langle T[a_{\boldsymbol{q}_1}^+(\tau_1) \\
&\quad \times a_{\boldsymbol{q}_2}^+(\tau_1) a_{\boldsymbol{q}_3}(\tau_1) a_{\boldsymbol{q}_4}(\tau_1) a_{\boldsymbol{q}_5}^+(\tau_2) a_{\boldsymbol{q}_6}^+(\tau_2) a_{\boldsymbol{q}_7}(\tau_2) a_{\boldsymbol{q}_8}(\tau_2) \\
&\quad \times a_{\boldsymbol{q}_9}^+(\tau_3) a_{\boldsymbol{q}_{10}}^+(\tau_3) a_{\boldsymbol{q}_{11}}(\tau_3) a_{\boldsymbol{q}_{12}}(\tau_3) a_{\boldsymbol{k}}(\tau) a_{\boldsymbol{k}}^+] \rangle_{\rm c}.
\end{aligned} \tag{4.4.1}$$

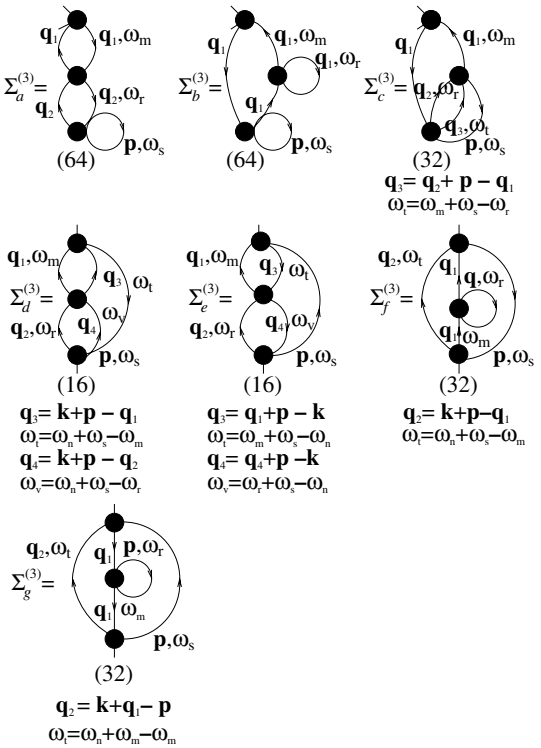

Fig. 4.3. Third-order irreducible diagrams in the frequency space. The multiplicity of each diagram is given by the number in brackets below the corresponding diagram.

The generalized Wick's theorem applied to Eq. (4.4.1) gives $7! = 5040$ fully contracted terms: of these $3! \times 328 = 1968$ lead to disconnected diagrams, $3! \times 256 = 1536$ lead to reducible connected diagrams and $3! \times 256 = 1536$ lead to irreducible connected diagrams. According to the vii) rule, the number of topologically non-equivalent diagrams is reduced by a factor 3!. Finally, using the invariance property of the interaction potential (4.1.6b), the 256 irreducible topologically non-equivalent, connected diagrams may be grouped into 7 classes of diagrams (in the frequency space) shown in Fig. 4.3. The third-order frequency Green function obtained from Eq. (4.4.1) becomes

$$\mathcal{G}^{(3)}_{\boldsymbol{k}}(i\omega_n) = [\mathcal{G}^{(0)}_{\boldsymbol{k}}(i\omega_n)]^2 \, [\Sigma^{(3)}_{\rm red}(\boldsymbol{k}, i\omega_n) + \Sigma^{(3)*}(\boldsymbol{k}, i\omega_n)] \tag{4.4.2}$$

where $\Sigma^{(3)}_{\rm red}$ is the third-order reducible self-energy and $\Sigma^{(3)*}$ is the third-order proper self-energy given by

$$\Sigma^{(3)*}(\boldsymbol{k}, i\omega_n) = \Sigma^{(3)}_a + \Sigma^{(3)}_b + \Sigma^{(3)}_c + \Sigma^{(3)}_d + \Sigma^{(3)}_e + \Sigma^{(3)}_f + \Sigma^{(3)}_g \tag{4.4.3}$$

where the self-energies occurring in Eq. (4.4.3) are shown in Fig. 4.3. According to the i)–viii) rules, we obtain the analytic form of each self-energy diagram shown in Fig. 4.3.

The self-energy $\Sigma_a^{(3)}$ is given by

$$\Sigma_a^{(3)}(\boldsymbol{k}, i\omega_n) = -\frac{64}{\hbar^3} \sum_{\boldsymbol{q}_1,\boldsymbol{q}_2,\boldsymbol{p}} V_{\boldsymbol{k},\boldsymbol{q}_1,\boldsymbol{k},\boldsymbol{q}_1} V_{\boldsymbol{q}_1,\boldsymbol{q}_2,\boldsymbol{q}_1,\boldsymbol{q}_2} V_{\boldsymbol{q}_2,\boldsymbol{p},\boldsymbol{q}_2,\boldsymbol{p}}$$
$$\times \frac{1}{\beta\hbar} \sum_m \frac{1}{(i\omega_m - \omega_{\boldsymbol{q}_1})^2} \; \frac{1}{\beta\hbar} \sum_r \frac{1}{(i\omega_r - \omega_{\boldsymbol{q}_2})^2} \; \frac{1}{\beta\hbar} \sum_s \frac{e^{i\omega_s \eta}}{i\omega_s - \omega_{\boldsymbol{p}}}. \tag{4.4.4}$$

By means of Eqs. (4.3.6) and (4.3.7), the self-energy (4.4.4) becomes

$$\Sigma_a^{(3)}(\boldsymbol{k}) = -4\beta \sum_{\boldsymbol{q}_1} V_{\boldsymbol{k},\boldsymbol{q}_1,\boldsymbol{k},\boldsymbol{q}_1} n_{\boldsymbol{q}_1}^{(0)} (1 + n_{\boldsymbol{q}_1}^{(0)}) \; \Sigma_b^{(2)}(\boldsymbol{q}_1). \tag{4.4.5}$$

In order to obtain the main temperature contribution to $\Sigma_a^{(3)}(\boldsymbol{k})$ in Eq. (4.4.5), we replace the temperature dependence of $\Sigma_b^{(2)}$ given by Eq. (3.6.9) and the interaction potential (4.1.6b). For a SC lattice, one has

$$\Sigma_a^{(3)}(\boldsymbol{k}) = -\frac{15}{4}\pi \left[\zeta\left(\frac{5}{2}\right)\right]^2 \frac{\omega_{\boldsymbol{k}}}{S^3} \left(\frac{k_B T}{8\pi J S}\right)^4 \frac{1}{N} \sum_{\boldsymbol{q}_1} (1 - \gamma_{\boldsymbol{q}_1})^2 n_{\boldsymbol{q}_1}^{(0)} (1 + n_{\boldsymbol{q}_1}^{(0)})$$
$$= -\frac{25}{4} \left[\pi \; \zeta\left(\frac{5}{2}\right)\right]^3 \frac{\omega_{\boldsymbol{k}}}{S^3} \left(\frac{k_B T}{8\pi J S}\right)^{\frac{15}{2}} \tag{4.4.6}$$

where we have used the relationship[3]

$$\frac{1}{N} \sum_{\boldsymbol{q}_1} (1 - \gamma_{\boldsymbol{q}_1})^2 n_{\boldsymbol{q}_1}^{(0)} (1 + n_{\boldsymbol{q}_1}^{(0)}) = \frac{1}{72\pi^2} \int_0^\infty dq_1 q_1^6 \frac{e^{2JSq_1^2}}{\left(e^{2JSq_1^2} - 1\right)^2}$$
$$= \left(\frac{k_B T}{2JS}\right)^{\frac{7}{2}} \frac{1}{144\pi^2} \int_0^\infty dx \frac{x^{5/2} \; e^x}{(e^x - 1)^2}$$
$$= \frac{5}{3}\pi^2 \zeta\left(\frac{5}{2}\right) \left(\frac{k_B T}{8\pi J S}\right)^{\frac{7}{2}}.$$

As one can see from Eq. (4.4.6), $\Sigma_a^{(3)}$ is a real function of the wavevector independent of the frequency and proportional to $T^{15/2}$. Therefore, the self-energy $\Sigma_a^{(3)}$ is negligible with respect to the first-order contribution $\Sigma^{(1)}$ propotional to $T^{5/2}$.

The self-energy $\Sigma_b^{(3)}$ is given by

$$\Sigma_b^{(3)}(\boldsymbol{k}) = -\frac{64}{\hbar^3} \sum_{\boldsymbol{q}_1,\boldsymbol{q},\boldsymbol{p}} V_{\boldsymbol{k},\boldsymbol{q}_1,\boldsymbol{k},\boldsymbol{q}_1} V_{\boldsymbol{q}_1,\boldsymbol{q},\boldsymbol{q}_1,\boldsymbol{q}} V_{\boldsymbol{q}_1,\boldsymbol{p},\boldsymbol{q}_1,\boldsymbol{p}}$$
$$\times \frac{1}{\beta\hbar} \sum_m \frac{1}{(i\omega_m - \omega_{\boldsymbol{q}_1})^3} \; \frac{1}{\beta\hbar} \sum_r \frac{e^{i\omega_r \eta}}{i\omega_r - \omega_{\boldsymbol{q}}} \; \frac{1}{\beta\hbar} \sum_s \frac{e^{i\omega_s \eta}}{i\omega_s - \omega_{\boldsymbol{p}}}. \tag{4.4.7}$$

To evaluate the sum over m, we introduce the meromorphic function

$$f_3(z) = \frac{1}{e^{\beta\hbar z} - 1} \; \frac{1}{(z - \omega_{\boldsymbol{q}_1})^3} \tag{4.4.8}$$

that vanishes on the circle Γ of radius $|z| \to \infty$ at least as $\frac{1}{z^3}$. Making use of the residue theorem around the circle Γ, one obtains

$$\frac{1}{\beta\hbar} \sum_r \frac{1}{(i\omega_r - \omega_{\boldsymbol{q}_1})^3} = -\frac{1}{2} (\beta\hbar)^2 \, n^{(0)}_{\boldsymbol{q}_1}(1 + n^{(0)}_{\boldsymbol{q}_1})(1 + 2n^{(0)}_{\boldsymbol{q}_1}). \tag{4.4.9}$$

From Eqs. (4.4.9) and (4.2.16), the self-energy $\Sigma^{(3)}_b$ becomes

$$\Sigma^{(3)}_b(\boldsymbol{k}) = 2\beta^2\hbar \sum_{\boldsymbol{q}_1} V_{\boldsymbol{k},\boldsymbol{q}_1,\boldsymbol{k},\boldsymbol{q}_1} \; n^{(0)}_{\boldsymbol{q}_1}(1 + n^{(0)}_{\boldsymbol{q}_1})(1 + 2 \; n^{(0)}_{\boldsymbol{q}_1}) \left[\Sigma^{(1)}(\boldsymbol{q}_1)\right]^2. \tag{4.4.10}$$

By means of Eqs. (3.6.2), (3.6.6), (4.1.6a) and (4.1.6b), one obtains

$$\begin{aligned}
\Sigma^{(3)}_b(\boldsymbol{k}) &= -\frac{9}{8} \; \frac{\omega_{\boldsymbol{k}}}{S^3} \left[\zeta\left(\frac{5}{2}\right)\right]^2 \left(\frac{k_B T}{8\pi J S}\right)^3 \frac{1}{N} \\
&\quad \times \sum_{\boldsymbol{q}_1} (1 - \gamma_{\boldsymbol{q}_1})^3 \; n^{(0)}_{\boldsymbol{q}_1}(1 + n^{(0)}_{\boldsymbol{q}_1})(1 + 2 \; n^{(0)}_{\boldsymbol{q}_1}) \\
&= -\frac{2}{3} \; \frac{\omega_{\boldsymbol{k}}}{S^3} \pi^{5/2} \left[\zeta\left(\frac{5}{2}\right)\right]^2 \left(\frac{k_B T}{8\pi J S}\right)^{\frac{15}{2}} \int_0^\infty dx \frac{x^{7/2} \; e^x(e^x + 1)}{(e^x - 1)^3} \\
&= -\frac{35}{8} \left[\pi\zeta\left(\frac{5}{2}\right)\right]^3 \frac{\omega_{\boldsymbol{k}}}{S^3} \left(\frac{k_B T}{8\pi J S}\right)^{\frac{15}{2}}
\end{aligned} \tag{4.4.11}$$

where we have used the relationship[3]

$$\int_0^\infty dx \frac{x^{7/2} \; e^x(e^x + 1)}{(e^x - 1)^3} = \frac{105}{16}\sqrt{\pi} \; \zeta\left(\frac{5}{2}\right).$$

From Eq. (4.4.11), one can see that $\Sigma^{(3)}_b$ is real and proportional to $T^{15/2}$ like $\Sigma^{(3)}_a$, negligible with respect to the first-order self-energy $\Sigma^{(1)}$.

The self-energy $\Sigma^{(3)}_c$ is given by

$$\begin{aligned}
\Sigma^{(3)}_c(\boldsymbol{k}) &= -\frac{32}{\hbar^3} \sum_{\boldsymbol{q}_1,\boldsymbol{q}_2,\boldsymbol{q}_3,\boldsymbol{p}} V_{\boldsymbol{k},\boldsymbol{q}_1,\boldsymbol{k},\boldsymbol{q}_1} V_{\boldsymbol{q}_1,\boldsymbol{p},\boldsymbol{q}_2,\boldsymbol{q}_3} V_{\boldsymbol{q}_2,\boldsymbol{q}_3,\boldsymbol{q}_1,\boldsymbol{p}} \; \frac{1}{\beta\hbar} \sum_m \frac{1}{(i\omega_m - \omega_{\boldsymbol{q}_1})^2} \\
&\quad \times \frac{1}{\beta\hbar} \sum_r \frac{1}{i\omega_r - \omega_{\boldsymbol{q}_2}} \; \frac{1}{\beta\hbar} \sum_s \frac{1}{i\omega_s - \omega_{\boldsymbol{p}}} \; \frac{1}{i\omega_m + i\omega_s - i\omega_r - \omega_{\boldsymbol{q}_3}} \\
&= \frac{4}{\hbar} \sum_{\boldsymbol{q}_1} V_{\boldsymbol{k},\boldsymbol{q}_1,\boldsymbol{k},\boldsymbol{q}_1} \; \frac{1}{\beta\hbar} \sum_m \frac{1}{(i\omega_m - \omega_{\boldsymbol{q}_1})^2} \; \Sigma^{(2)}_c(\boldsymbol{q}_1, i\omega_m)
\end{aligned} \tag{4.4.12}$$

where we have used Eq. (4.3.10). From Eq. (4.3.16), we obtain

$$\Sigma_c^{(3)}(\boldsymbol{k}) = -\frac{32}{\hbar^3}\sum_{\boldsymbol{q}_1,\boldsymbol{q}_2,\boldsymbol{q}_3,\boldsymbol{p}} V_{\boldsymbol{k},\boldsymbol{q}_1,\boldsymbol{k},\boldsymbol{q}_1} V_{\boldsymbol{q}_1,\boldsymbol{p},\boldsymbol{q}_2,\boldsymbol{q}_3} V_{\boldsymbol{q}_2,\boldsymbol{q}_3,\boldsymbol{q}_1,\boldsymbol{p}}$$
$$\times\left[n_{\boldsymbol{p}}^{(0)}(1+n_{\boldsymbol{q}_2}^{(0)}+n_{\boldsymbol{q}_3}^{(0)}) - n_{\boldsymbol{q}_2}^{(0)}n_{\boldsymbol{q}_3}^{(0)}\right]$$
$$\times\frac{1}{\beta\hbar}\sum_m \frac{1}{(i\omega_m-\omega_{\boldsymbol{q}_1})^2}\ \frac{1}{i\omega_m-\omega_{\boldsymbol{q}_2}-\omega_{\boldsymbol{q}_3}+\omega_{\boldsymbol{p}}}. \qquad (4.4.13)$$

To evaluate the sum over m in Eq. (4.4.13), we may proceed in a way similar to that used in Eq. (4.3.12) or introducing a meromorphic function $f_4(z)$ given by

$$f_4(z) = \frac{1}{e^{\beta\hbar z}-1}\ \frac{1}{(z-\omega_{\boldsymbol{q}_1})^2}\ \frac{1}{z-\omega_{\boldsymbol{q}_2}-\omega_{\boldsymbol{q}_3}+\omega_{\boldsymbol{q}_4}} \qquad (4.4.14)$$

and using the residue theorem around a circle Γ with $|z|\to\infty$ on which the function $f_4(z)$ vanishes at least as $\frac{1}{z^3}$. Both procedures lead to the relationship

$$\frac{1}{\beta\hbar}\sum_m \frac{1}{(i\omega_m-\omega_{\boldsymbol{q}_1})^2}\ \frac{1}{i\omega_m-\omega_{\boldsymbol{q}_2}-\omega_{\boldsymbol{q}_3}+\omega_{\boldsymbol{p}}}$$
$$= \frac{\beta\hbar\ n_{\boldsymbol{q}_1}^{(0)}(1+n_{\boldsymbol{q}_1}^{(0)})}{\omega_{\boldsymbol{q}_1}-\omega_{\boldsymbol{q}_2}-\omega_{\boldsymbol{q}_3}+\omega_{\boldsymbol{p}}} + \frac{1}{(\omega_{\boldsymbol{q}_1}-\omega_{\boldsymbol{q}_2}-\omega_{\boldsymbol{q}_3}+\omega_{\boldsymbol{p}})^2}$$
$$\times\frac{n_{\boldsymbol{q}_1}^{(0)}n_{\boldsymbol{p}}^{(0)}(1+n_{\boldsymbol{q}_2}^{(0)}+n_{\boldsymbol{q}_3}^{(0)}) - n_{\boldsymbol{q}_2}^{(0)}n_{\boldsymbol{q}_3}^{(0)}(1+n_{\boldsymbol{q}_1}^{(0)}+n_{\boldsymbol{p}}^{(0)})}{n_{\boldsymbol{p}}^{(0)}(1+n_{\boldsymbol{q}_2}^{(0)}+n_{\boldsymbol{q}_3}^{(0)}) - n_{\boldsymbol{q}_2}^{(0)}n_{\boldsymbol{q}_3}^{(0)}}. \qquad (4.4.15)$$

Replacing Eq. (4.4.15) into Eq. (4.4.13), one obtains

$$\Sigma_c^{(3)}(\boldsymbol{k}) = -\frac{32}{\hbar^3}\sum_{\boldsymbol{q}_1,\boldsymbol{q}_2,\boldsymbol{q}_3,\boldsymbol{p}} V_{\boldsymbol{q}_1,\boldsymbol{p},\boldsymbol{q}_2,\boldsymbol{q}_3} V_{\boldsymbol{q}_2,\boldsymbol{q}_3,\boldsymbol{q}_1,\boldsymbol{p}}\ \frac{1}{\omega_{\boldsymbol{q}_1}-\omega_{\boldsymbol{q}_2}-\omega_{\boldsymbol{q}_3}+\omega_{\boldsymbol{p}}}$$
$$\times\Bigg\{\beta\hbar\ V_{\boldsymbol{k},\boldsymbol{q}_1,\boldsymbol{k},\boldsymbol{q}_1}\ n_{\boldsymbol{q}_1}^{(0)}(1+n_{\boldsymbol{q}_1}^{(0)})\left[n_{\boldsymbol{p}}^{(0)}(1+n_{\boldsymbol{q}_2}^{(0)}+n_{\boldsymbol{q}_3}^{(0)}) - n_{\boldsymbol{q}_2}^{(0)}n_{\boldsymbol{q}_3}^{(0)}\right]$$
$$+ (V_{\boldsymbol{k},\boldsymbol{q}_1,\boldsymbol{k},\boldsymbol{q}_1} - V_{\boldsymbol{k},\boldsymbol{q}_2,\boldsymbol{k},\boldsymbol{q}_2})\frac{n_{\boldsymbol{q}_1}^{(0)}n_{\boldsymbol{p}}^{(0)}(1+n_{\boldsymbol{q}_2}^{(0)}+n_{\boldsymbol{q}_3}^{(0)})}{\omega_{\boldsymbol{q}_1}-\omega_{\boldsymbol{q}_2}-\omega_{\boldsymbol{q}_3}+\omega_{\boldsymbol{p}}}\Bigg\}.. \qquad (4.4.16)$$

The self-energy $\Sigma_d^{(3)}$ is given by

$$\Sigma_d^{(3)}(\boldsymbol{k}, i\omega_n) = -\frac{16}{\hbar^3}\sum_{\boldsymbol{q}_1,\boldsymbol{q}_2,\boldsymbol{q}_3,\boldsymbol{q}_4,\boldsymbol{p}} V_{\boldsymbol{k},\boldsymbol{p},\boldsymbol{q}_1,\boldsymbol{q}_3} V_{\boldsymbol{q}_1,\boldsymbol{q}_3,\boldsymbol{q}_2,\boldsymbol{q}_4} V_{\boldsymbol{q}_2,\boldsymbol{q}_4,\boldsymbol{k},\boldsymbol{p}}\ \frac{1}{\beta\hbar}\sum_s \frac{1}{i\omega_s-\omega_{\boldsymbol{p}}}$$
$$\times\frac{1}{\beta\hbar}\sum_m \frac{1}{i\omega_m-\omega_{\boldsymbol{q}_1}}\ \frac{1}{i\omega_n+i\omega_s-i\omega_m-\omega_{\boldsymbol{q}_3}}$$

$$\times\frac{1}{\beta\hbar}\sum_r \frac{1}{i\omega_r-\omega_{\boldsymbol{q}_2}}\ \frac{1}{i\omega_n+i\omega_s-i\omega_r-\omega_{\boldsymbol{q}_4}}$$

$$=-\frac{16}{\hbar^3}\sum_{\boldsymbol{q}_1,\boldsymbol{q}_2,\boldsymbol{q}_3,\boldsymbol{q}_4,\boldsymbol{p}} V_{\boldsymbol{k},\boldsymbol{p},\boldsymbol{q}_1,\boldsymbol{q}_3}V_{\boldsymbol{q}_1,\boldsymbol{q}_2,\boldsymbol{q}_2,\boldsymbol{q}_4}V_{\boldsymbol{q}_2,\boldsymbol{q}_4,\boldsymbol{k},\boldsymbol{p}}\ \frac{1}{\beta\hbar}\sum_s \frac{1}{i\omega_s-\omega_{\boldsymbol{p}}}$$

$$\times\frac{1+n^{(0)}_{\boldsymbol{q}_1}+n^{(0)}_{\boldsymbol{q}_3}}{i\omega_n+i\omega_s-\omega_{\boldsymbol{q}_1}-\omega_{\boldsymbol{q}_3}}\ \frac{1+n^{(0)}_{\boldsymbol{q}_2}+n^{(0)}_{\boldsymbol{q}_4}}{i\omega_n+i\omega_s-\omega_{\boldsymbol{q}_2}-\omega_{\boldsymbol{q}_4}} \tag{4.4.17}$$

where the sums over m and r have been performed using Eq. (4.3.11). The sum over s can be performed in a similar way leading to

$$\Sigma^{(3)}_d(\boldsymbol{k},i\omega_n)=\frac{16}{\hbar^3}\sum_{\boldsymbol{q}_1,\boldsymbol{q}_2,\boldsymbol{q}_3,\boldsymbol{q}_4,\boldsymbol{p}} V_{\boldsymbol{k},\boldsymbol{p},\boldsymbol{q}_1,\boldsymbol{q}_3}V_{\boldsymbol{q}_1,\boldsymbol{q}_3,\boldsymbol{q}_2,\boldsymbol{q}_4}V_{\boldsymbol{q}_2,\boldsymbol{q}_4,\boldsymbol{k},\boldsymbol{p}}\ \frac{1}{\omega_{\boldsymbol{q}_1}+\omega_{\boldsymbol{q}_3}-\omega_{\boldsymbol{q}_2}-\omega_{\boldsymbol{q}_4}}$$

$$\times\left[(1+n^{(0)}_{\boldsymbol{q}_2}+n^{(0)}_{\boldsymbol{q}_4})\frac{n^{(0)}_{\boldsymbol{p}}(1+n^{(0)}_{\boldsymbol{q}_1}+n^{(0)}_{\boldsymbol{q}_3})-n^{(0)}_{\boldsymbol{q}_1}n^{(0)}_{\boldsymbol{q}_3}}{i\omega_n-\omega_{\boldsymbol{q}_1}-\omega_{\boldsymbol{q}_3}+\omega_{\boldsymbol{p}}}\right.$$

$$\left.-(1+n^{(0)}_{\boldsymbol{q}_1}+n^{(0)}_{\boldsymbol{q}_3})\frac{n^{(0)}_{\boldsymbol{p}}(1+n^{(0)}_{\boldsymbol{q}_2}+n^{(0)}_{\boldsymbol{q}_4})-n^{(0)}_{\boldsymbol{q}_2}n^{(0)}_{\boldsymbol{q}_4}}{i\omega_n-\omega_{\boldsymbol{q}_2}-\omega_{\boldsymbol{q}_4}+\omega_{\boldsymbol{p}}}\right]. \tag{4.4.18}$$

The self-energy $\Sigma^{(3)}_e$ is given by

$$\Sigma^{(3)}_e(\boldsymbol{k},i\omega_n)=-\frac{16}{\hbar^3}\sum_{\boldsymbol{q}_1,\boldsymbol{q}_2,\boldsymbol{q}_3,\boldsymbol{q}_4,\boldsymbol{p}} V_{\boldsymbol{k},\boldsymbol{q}_3,\boldsymbol{q}_1,\boldsymbol{p}}V_{\boldsymbol{q}_1,\boldsymbol{q}_4,\boldsymbol{q}_2,\boldsymbol{q}_3}V_{\boldsymbol{q}_2,\boldsymbol{p},\boldsymbol{k},\boldsymbol{q}_4}$$

$$\times\frac{1}{\beta\hbar}\sum_s \frac{1}{i\omega_s-\omega_{\boldsymbol{p}}}\frac{1}{\beta\hbar}\sum_m \frac{1}{i\omega_m-\omega_{\boldsymbol{q}_1}}\ \frac{1}{i\omega_m+i\omega_s-i\omega_n-\omega_{\boldsymbol{q}_3}}$$

$$\times\frac{1}{\beta\hbar}\sum_r \frac{1}{i\omega_r-\omega_{\boldsymbol{q}_2}}\ \frac{1}{i\omega_r+i\omega_s-i\omega_n-\omega_{\boldsymbol{q}_4}}$$

$$=-\frac{16}{\hbar^3}\sum_{\boldsymbol{q}_1,\boldsymbol{q}_2,\boldsymbol{q}_3,\boldsymbol{q}_4,\boldsymbol{p}} V_{\boldsymbol{k},\boldsymbol{q}_3,\boldsymbol{q}_1,\boldsymbol{p}}V_{\boldsymbol{q}_1,\boldsymbol{q}_4,\boldsymbol{q}_2,\boldsymbol{q}_3}V_{\boldsymbol{q}_2,\boldsymbol{p},\boldsymbol{k},\boldsymbol{q}_4}$$

$$\times(n^{(0)}_{\boldsymbol{q}_1}-n^{(0)}_{\boldsymbol{q}_3})(n^{(0)}_{\boldsymbol{q}_2}-n^{(0)}_{\boldsymbol{q}_4})\frac{1}{\beta\hbar}\sum_s \frac{1}{i\omega_s-\omega_{\boldsymbol{p}}}$$

$$\times\frac{1}{i\omega_s-i\omega_n+\omega_{\boldsymbol{q}_1}-\omega_{\boldsymbol{q}_3}}\ \frac{1}{i\omega_s-i\omega_n+\omega_{\boldsymbol{q}_2}-\omega_{\boldsymbol{q}_4}}. \tag{4.4.19}$$

The sums over m and r in Eq. (4.4.19) have been performed using the relationship

$$\frac{1}{\beta\hbar}\sum_m \frac{1}{i\omega_m-\omega_{\boldsymbol{q}_1}}\ \frac{1}{i\omega_m+i\omega_s-i\omega_n-\omega_{\boldsymbol{q}_3}}=\frac{n^{(0)}_{\boldsymbol{q}_3}-n^{(0)}_{\boldsymbol{q}_1}}{i\omega_s-i\omega_n+\omega_{\boldsymbol{q}_1}-\omega_{\boldsymbol{q}_3}} \tag{4.4.20}$$

obtained in a way similar to that used to write Eq. (4.3.11). The remaining sum over s in Eq. (4.4.19) may be performed using an analogous procedure. One obtains

$$\Sigma_e^{(3)}(\boldsymbol{k}, i\omega_n) = \frac{16}{\hbar^3} \sum_{\boldsymbol{q}_1,\boldsymbol{q}_2,\boldsymbol{q}_3,\boldsymbol{q}_4,\boldsymbol{p}} \big(V_{\boldsymbol{k},\boldsymbol{q}_3,\boldsymbol{q}_1,\boldsymbol{p}} V_{\boldsymbol{q}_1,\boldsymbol{q}_4,\boldsymbol{q}_2,\boldsymbol{q}_3} V_{\boldsymbol{q}_2,\boldsymbol{p},\boldsymbol{k},\boldsymbol{q}_4} + V_{\boldsymbol{q}_4,\boldsymbol{k},\boldsymbol{p},\boldsymbol{q}_2} V_{\boldsymbol{q}_3,\boldsymbol{q}_2,\boldsymbol{q}_4,\boldsymbol{q}_1} V_{\boldsymbol{p},\boldsymbol{q}_1,\boldsymbol{q}_3,\boldsymbol{k}}\big) \frac{n_{\boldsymbol{q}_1}^{(0)} - n_{\boldsymbol{q}_3}^{(0)}}{\omega_{\boldsymbol{q}_2} + \omega_{\boldsymbol{q}_3} - \omega_{\boldsymbol{q}_1} - \omega_{\boldsymbol{q}_4}} \times \frac{n_{\boldsymbol{p}}^{(0)}(n_{\boldsymbol{q}_2}^{(0)} - n_{\boldsymbol{q}_4}^{(0)}) - n_{\boldsymbol{q}_4}^{(0)}(1 + n_{\boldsymbol{q}_2}^{(0)})}{i\omega_n + \omega_{\boldsymbol{q}_4} - \omega_{\boldsymbol{q}_2} - \omega_{\boldsymbol{p}}}. \tag{4.4.21}$$

The self-energy $\Sigma_f^{(3)}$ is given by

$$\begin{aligned}\Sigma_f^{(3)}(\boldsymbol{k}, i\omega_n) &= -\frac{32}{\hbar^3} \sum_{\boldsymbol{q}_1,\boldsymbol{q}_2,\boldsymbol{q}_3,\boldsymbol{p}} V_{\boldsymbol{k},\boldsymbol{p},\boldsymbol{q}_1,\boldsymbol{q}_2} V_{\boldsymbol{q}_1,\boldsymbol{q},\boldsymbol{q}_1,\boldsymbol{q}} V_{\boldsymbol{q}_1,\boldsymbol{q}_2,\boldsymbol{k},\boldsymbol{p}} \; \frac{1}{\beta\hbar} \sum_r \frac{e^{i\omega_r \eta}}{i\omega_r - \omega_{\boldsymbol{q}}} \\ &\quad \times \frac{1}{\beta\hbar} \sum_m \frac{1}{(i\omega_m - \omega_{\boldsymbol{q}_1})^2} \; \frac{1}{\beta\hbar} \sum_s \frac{1}{i\omega_s - \omega_{\boldsymbol{p}}} \; \frac{1}{i\omega_s + i\omega_n - i\omega_m - \omega_{\boldsymbol{q}_2}} \\ &= \frac{8}{\hbar^2} \sum_{\boldsymbol{q}_1,\boldsymbol{q}_2,\boldsymbol{p}} V_{\boldsymbol{k},\boldsymbol{p},\boldsymbol{q}_1,\boldsymbol{q}_2} V_{\boldsymbol{q}_1,\boldsymbol{q}_2,\boldsymbol{k},\boldsymbol{p}} \; \Sigma^{(1)}(\boldsymbol{q}_1) \; (n_{\boldsymbol{q}_2}^{(0)} - n_{\boldsymbol{p}}^{(0)}) \\ &\quad \times \frac{1}{\beta\hbar} \sum_m \frac{1}{(i\omega_m - \omega_{\boldsymbol{q}_1})^2} \; \frac{1}{i\omega_n - i\omega_m - \omega_{\boldsymbol{q}_2} + \omega_{\boldsymbol{p}}}\end{aligned} \tag{4.4.22}$$

where Eq. (4.2.10) has been used and the sum over s is taken from Eq. (4.4.20). Moreover,

$$\begin{aligned}&\frac{1}{\beta\hbar} \sum_m \frac{1}{(i\omega_m - \omega_{\boldsymbol{q}_1})^2} \; \frac{1}{i\omega_n - i\omega_m - \omega_{\boldsymbol{q}_2} + \omega_{\boldsymbol{p}}} \\ &\quad = \frac{\beta\hbar \; n_{\boldsymbol{q}_1}^{(0)}(1 + n_{\boldsymbol{q}_1}^{(0)})}{i\omega_n + \omega_{\boldsymbol{p}} - \omega_{\boldsymbol{q}_1} - \omega_{\boldsymbol{q}_2}} + \frac{1}{(i\omega_n + \omega_{\boldsymbol{p}} - \omega_{\boldsymbol{q}_1} - \omega_{\boldsymbol{q}_2})^2} \\ &\qquad \times \frac{n_{\boldsymbol{p}}^{(0)}(1 + n_{\boldsymbol{q}_2}^{(0)}) - n_{\boldsymbol{q}_1}^{(0)}(n_{\boldsymbol{q}_2}^{(0)} - n_{\boldsymbol{p}}^{(0)})}{n_{\boldsymbol{q}_2}^{(0)} - n_{\boldsymbol{p}}^{(0)}}.\end{aligned} \tag{4.4.23}$$

Replacing Eq. (4.4.23) into Eq. (4.4.22), one obtains

$$\begin{aligned}\Sigma_f^{(3)}(\boldsymbol{k}, i\omega_n) &= \frac{8}{\hbar^2} \sum_{\boldsymbol{q}_1,\boldsymbol{q}_2,\boldsymbol{p}} V_{\boldsymbol{k},\boldsymbol{p},\boldsymbol{q}_1,\boldsymbol{q}_2} V_{\boldsymbol{q}_1,\boldsymbol{q}_2,\boldsymbol{k},\boldsymbol{p}} \; \Sigma^{(1)}(\boldsymbol{q}_1) \\ &\quad \times \Bigg[\beta\hbar \; \frac{n_{\boldsymbol{q}_1}^{(0)}(1 + n_{\boldsymbol{q}_1}^{(0)})(n_{\boldsymbol{q}_2}^{(0)} - n_{\boldsymbol{p}}^{(0)})}{i\omega_n + \omega_{\boldsymbol{p}} - \omega_{\boldsymbol{q}_1} - \omega_{\boldsymbol{q}_2}} \\ &\qquad + \frac{n_{\boldsymbol{p}}^{(0)}(1 + n_{\boldsymbol{q}_2}^{(0)}) - n_{\boldsymbol{q}_1}(n_{\boldsymbol{q}_2}^{(0)} - n_{\boldsymbol{p}}^{(0)})}{(i\omega_n + \omega_{\boldsymbol{p}} - \omega_{\boldsymbol{q}_1} - \omega_{\boldsymbol{q}_2})^2}\Bigg].\end{aligned} \tag{4.4.24}$$

The self-energy $\Sigma_g^{(3)}$ is given by

$$\Sigma_g^{(3)}(\boldsymbol{k}, i\omega_n) = -\frac{32}{\hbar^3} \sum_{\boldsymbol{q}_1,\boldsymbol{q}_2,\boldsymbol{q},\boldsymbol{p}} V_{\boldsymbol{k},\boldsymbol{q}_1,\boldsymbol{q}_2,\boldsymbol{p}} V_{\boldsymbol{q}_1,\boldsymbol{q},\boldsymbol{q}_1,\boldsymbol{q}} V_{\boldsymbol{q}_2,\boldsymbol{p},\boldsymbol{k},\boldsymbol{q}_1} \frac{1}{\beta\hbar} \sum_r \frac{e^{i\omega_r\eta}}{i\omega_r - \omega_{\boldsymbol{q}}}$$

$$\times \frac{1}{\beta\hbar} \sum_m \frac{1}{(i\omega_m - \omega_{\boldsymbol{q}_1})^2} \frac{1}{\beta\hbar} \sum_s \frac{1}{i\omega_s - \omega_{\boldsymbol{p}}} \frac{1}{i\omega_m + i\omega_n - i\omega_s - \omega_{\boldsymbol{q}_2}}$$

$$= -\frac{8}{\hbar^2} \sum_{\boldsymbol{q}_1,\boldsymbol{q}_2,\boldsymbol{p}} V_{\boldsymbol{k},\boldsymbol{q}_1,\boldsymbol{q}_2,\boldsymbol{p}} V_{\boldsymbol{q}_2,\boldsymbol{p},\boldsymbol{k},\boldsymbol{q}_1} \Sigma^{(1)}(\boldsymbol{q}_1)\ (1 + n_{\boldsymbol{p}}^{(0)} + n_{\boldsymbol{q}_2}^{(0)})$$

$$\times \frac{1}{\beta\hbar} \sum_m \frac{1}{(i\omega_m - \omega_{\boldsymbol{q}_1})^2} \frac{1}{i\omega_m + i\omega_n - \omega_{\boldsymbol{q}_2} - \omega_{\boldsymbol{p}}} \tag{4.4.25}$$

where Eq. (4.2.10) has been used and the sum over s is taken from Eq. (4.3.11). Using the relationship

$$\frac{1}{\beta\hbar} \sum_m \frac{1}{(i\omega_m - \omega_{\boldsymbol{q}_1})^2} \frac{1}{i\omega_m + i\omega_n - \omega_{\boldsymbol{q}_2} - \omega_{\boldsymbol{p}}}$$

$$= \frac{\beta\hbar\ n_{\boldsymbol{q}_1}^{(0)}(1 + n_{\boldsymbol{q}_1}^{(0)})}{i\omega_n - \omega_{\boldsymbol{q}_2} - \omega_{\boldsymbol{p}} + \omega_{\boldsymbol{q}_1}} + \frac{1}{(i\omega_n - \omega_{\boldsymbol{q}_2} - \omega_{\boldsymbol{p}} + \omega_{\boldsymbol{q}_1})^2}$$

$$\times \frac{n_{\boldsymbol{q}_1}^{(0)}(1 + n_{\boldsymbol{q}_2}^{(0)} + n_{\boldsymbol{p}}^{(0)}) - n_{\boldsymbol{q}_2}^{(0)} n_{\boldsymbol{p}}^{(0)}}{1 + n_{\boldsymbol{q}_2}^{(0)} + n_{\boldsymbol{p}}^{(0)}} \tag{4.4.26}$$

the self-energy $\Sigma_g^{(3)}$ becomes

$$\Sigma_g^{(3)}(\boldsymbol{k}, i\omega_n) = -\frac{8}{\hbar^2} \sum_{\boldsymbol{q}_1,\boldsymbol{q}_2,\boldsymbol{p}} V_{\boldsymbol{k},\boldsymbol{q}_1,\boldsymbol{q}_2,\boldsymbol{p}} V_{\boldsymbol{q}_2,\boldsymbol{p},\boldsymbol{k},\boldsymbol{q}_1}\ \Sigma^{(1)}(\boldsymbol{q}_1)$$

$$\times \left[\frac{\beta\hbar\ n_{\boldsymbol{q}_1}^{(0)}(1 + n_{\boldsymbol{q}_1}^{(0)})(1 + n_{\boldsymbol{q}_2}^{(0)} + n_{\boldsymbol{p}}^{(0)})}{i\omega_n - \omega_{\boldsymbol{q}_2} - \omega_{\boldsymbol{p}} + \omega_{\boldsymbol{q}_1}} \right.$$

$$\left. + \frac{n_{\boldsymbol{q}_1}^{(0)}(1 + n_{\boldsymbol{q}_2}^{(0)} + n_{\boldsymbol{p}}^{(0)}) - n_{\boldsymbol{q}_2}^{(0)} n_{\boldsymbol{p}}^{(0)}}{(i\omega_n - \omega_{\boldsymbol{q}_2} - \omega_{\boldsymbol{p}} + \omega_{\boldsymbol{q}_1})^2} \right]. \tag{4.4.27}$$

4.5. T-matrix Approximation

As shown in the previous sections, the main temperature contributions to the proper self-energy come from the diagrams containing a single downward line like $\Sigma^{(1)}$ [see Fig. 4.1 and Eq. (4.2.10)], $\Sigma_c^{(2)}$ [see Fig. 4.2 and Eq. (4.3.13) or (4.3.16] and $\Sigma_d^{(3)}$ [see Fig. 4.3 and Eq. (4.4.17) or (4.4.18]. The peculiar shape of these diagrams suggests how to select *all* the infinite contributions to the lowest order in temperature. Indeed, in order to build a temperature series expansion, particularly useful to fit the experimental data at low temperature, one has to keep all diagrams containing only one downward line. Such diagrams look like a "ladder", the rungs of which

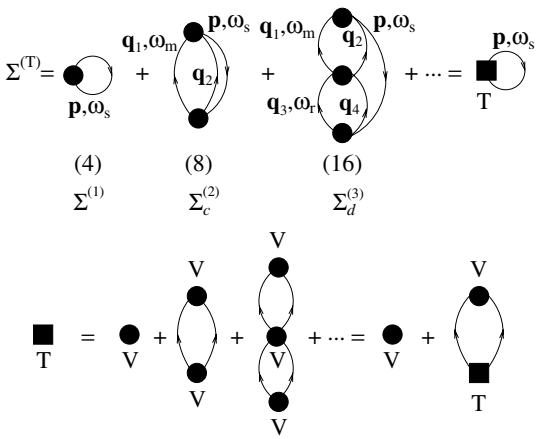

Fig. 4.4. T-matrix contribution to the self-energy (upper) and self-consistent equation for the T-matrix (lower). V is the interaction potential.

are the full circles representing the interaction potential. Each rung is connected to the next by a couple of upward lines except the highest and lowest rung that are connected by a downward line. The self-energy corresponding to the sum of such diagrams is called *T-matrix* self-energy and it is shown in Fig. 4.4 along with the T-matrix self-consistent equation. Analytically, the first few terms of the T-matrix self-energy are given by Eqs. (4.2.10), (4.3.13) and (4.4.17) that is

$$\begin{aligned}\Sigma^{(\mathrm{T})}(\boldsymbol{k}, i\omega_n) = \Sigma^{(1)}(\boldsymbol{k}) + \Sigma_c^{(2)}(\boldsymbol{k}, i\omega_n) + \Sigma_d^{(3)}(\boldsymbol{k}, i\omega_n) + \cdots = -2\sum_{\boldsymbol{p}} \frac{1}{\beta\hbar} \\ \times \sum_s \frac{1}{i\omega_s - \omega_{\boldsymbol{p}}} \Bigg[\frac{2}{\hbar}\, V_{\boldsymbol{k},\boldsymbol{p},\boldsymbol{k},\boldsymbol{p}} + \sum_{\boldsymbol{q}_1,\boldsymbol{q}_2} \left(\frac{2}{\hbar}\right)^2 V_{\boldsymbol{k},\boldsymbol{p},\boldsymbol{q}_1,\boldsymbol{q}_2} V_{\boldsymbol{q}_1,\boldsymbol{q}_2,\boldsymbol{k},\boldsymbol{p}} \\ \times \frac{1 + n^{(0)}_{\boldsymbol{q}_1} + n(0)_{\boldsymbol{q}_2}}{i\omega_s + i\omega_n - \omega_{\boldsymbol{q}_1} - \omega_{\boldsymbol{q}_2}} + \sum_{\boldsymbol{q}_1,\boldsymbol{q}_2,\boldsymbol{q}_3,\boldsymbol{q}_4} \left(\frac{2}{\hbar}\right)^3 V_{\boldsymbol{k},\boldsymbol{p},\boldsymbol{q}_1,\boldsymbol{q}_2} V_{\boldsymbol{q}_1,\boldsymbol{q}_2,\boldsymbol{q}_3,\boldsymbol{q}_4} \\ \times V_{\boldsymbol{q}_3,\boldsymbol{q}_4,\boldsymbol{k},\boldsymbol{p}} \frac{1 + n^{(0)}_{\boldsymbol{q}_1} + n^{(0)}_{\boldsymbol{q}_2}}{i\omega_s + i\omega_n - \omega_{\boldsymbol{q}_1} - \omega_{\boldsymbol{q}_2}} \; \frac{1 + n^{(0)}_{\boldsymbol{q}_3} + n^{(0)}_{\boldsymbol{q}_4}}{i\omega_s + i\omega_n - \omega_{\boldsymbol{q}_3} - \omega_{\boldsymbol{q}_4}} + \cdots \Bigg] \\ = -2\sum_{\boldsymbol{p}} \frac{1}{\beta\hbar} \sum_s \frac{1}{i\omega_s - \omega_{\boldsymbol{p}}} \; \frac{2}{\hbar}\, T_{\boldsymbol{k},\boldsymbol{p},\boldsymbol{k},\boldsymbol{p}}(i\omega_n + i\omega_s). \end{aligned} \tag{4.5.1}$$

From Eq. (4.5.1), one can obtain the self-consistent equation for the T-matrix

$$T_{\boldsymbol{q}_1,\boldsymbol{q}_2,\boldsymbol{q}_3,\boldsymbol{q}_4}(\omega) = V_{\boldsymbol{q}_1,\boldsymbol{q}_2,\boldsymbol{q}_3,\boldsymbol{q}_4} + \frac{2}{\hbar} \sum_{\boldsymbol{q}_5,\boldsymbol{q}_6} V_{\boldsymbol{q}_1,\boldsymbol{q}_2,\boldsymbol{q}_5,\boldsymbol{q}_6} \; \frac{1 + n^{(0)}_{\boldsymbol{q}_5} + n^{(0)}_{\boldsymbol{q}_6}}{\omega - \omega_{\boldsymbol{q}_5} - \omega_{\boldsymbol{q}_6}} \; T_{\boldsymbol{q}_5,\boldsymbol{q}_6,\boldsymbol{q}_3,\boldsymbol{q}_4}(\omega). \tag{4.5.2}$$

The δ-function occurring in the interaction potential of Eq. (4.1.6a) is satisfied by choosing $\boldsymbol{q}_1 = \frac{1}{2}\boldsymbol{K} + \boldsymbol{\lambda}$, $\boldsymbol{q}_2 = \frac{1}{2}\boldsymbol{K} - \boldsymbol{\lambda}$, $\boldsymbol{q}_3 = \frac{1}{2}\boldsymbol{K} + \boldsymbol{\mu}$, $\boldsymbol{q}_4 = \frac{1}{2}\boldsymbol{K} - \boldsymbol{\mu}$. Such a choice allows us to write the interaction potential (4.1.6a) as

$$\begin{aligned} V_{\boldsymbol{q}_1,\boldsymbol{q}_2,\boldsymbol{q}_3,\boldsymbol{q}_4} = V_{\boldsymbol{\lambda},\boldsymbol{\mu}}(\boldsymbol{K}) &= -\frac{zJ}{2N}(\gamma_{\boldsymbol{\lambda}-\boldsymbol{\mu}} + \gamma_{\boldsymbol{\lambda}+\boldsymbol{\mu}} - \gamma_{\frac{1}{2}\boldsymbol{K}+\boldsymbol{\lambda}} - \gamma_{\frac{1}{2}\boldsymbol{K}-\boldsymbol{\lambda}}) \\ &= -\frac{2J}{N}\sum_{\alpha}\cos\lambda_\alpha\left(\cos\mu_\alpha - \cos\frac{K_\alpha}{2}\right) \end{aligned} \tag{4.5.3}$$

where the lattice constant is assigned to be $a = 1$ and α runs over half of the NN: in a SC lattice, $\alpha = x, y, z$. The T-matrix self-consistent equation (4.5.2) becomes

$$T_{\boldsymbol{\lambda},\boldsymbol{\mu}}(\boldsymbol{K},\omega) = V_{\boldsymbol{\lambda},\boldsymbol{\mu}}(\boldsymbol{K}) + \frac{2}{\hbar}\sum_{\boldsymbol{\rho}} V_{\boldsymbol{\lambda},\boldsymbol{\rho}}(\boldsymbol{K})\,\frac{1 + n^{(0)}_{\frac{1}{2}\boldsymbol{K}+\boldsymbol{\rho}} + n^{(0)}_{\frac{1}{2}\boldsymbol{K}-\boldsymbol{\rho}}}{\omega - \omega_{\frac{1}{2}\boldsymbol{K}+\boldsymbol{\rho}} - \omega_{\frac{1}{2}\boldsymbol{K}-\boldsymbol{\rho}}}\,T_{\boldsymbol{\rho},\boldsymbol{\mu}}(\boldsymbol{K},\omega). \tag{4.5.4}$$

The solution of Eq. (4.5.4) is given by

$$T_{\boldsymbol{\lambda},\boldsymbol{\mu}}(\boldsymbol{K},\omega) = -\frac{2J}{N}\sum_{\alpha,\beta}\cos\lambda_\alpha\left[\mathbf{1} - \frac{1}{2S}\mathbf{B}(\boldsymbol{K},\omega)\right]^{-1}_{\alpha\beta}\left(\cos\mu_\beta - \cos\frac{K_\beta}{2}\right) \tag{4.5.5}$$

where $\mathbf{1}$ is the unit matrix and

$$\mathrm{B}_{\alpha\beta}(\boldsymbol{K},\omega) = \frac{1}{N}\sum_{\boldsymbol{\rho}}\frac{\left(\cos\frac{K_\alpha}{2} - \cos\rho_\alpha\right)\cos\rho_\beta}{x + \sum_\sigma \cos\frac{K_\sigma}{2}\cos\rho_\sigma}\left(1 + n^{(0)}_{\frac{1}{2}\boldsymbol{K}+\boldsymbol{\rho}} + n^{(0)}_{\frac{1}{2}\boldsymbol{K}-\boldsymbol{\rho}}\right) \tag{4.5.6}$$

with

$$x = \frac{\hbar\omega}{8JS} - \frac{z}{2}. \tag{4.5.7}$$

For a SC lattice, both $\mathbf{1}$ and $\mathbf{B}$ are 3×3 matrices and the 9 elements of the $\mathbf{B}$-matrix are given by Eq. (4.5.6) with $\alpha, \beta = x, y, z$. Note that Eq. (4.5.5) involves the elements of the *inverse* matrix of ($\mathbf{1}$-$\frac{1}{2S}\mathbf{B}$). The T-matrix self-energy of Eq. (4.5.1) becomes

$$\Sigma^{(\mathrm{T})}(\boldsymbol{k}, i\omega_n) = -\frac{4}{\hbar}\sum_{\boldsymbol{p}}\frac{1}{\beta\hbar}\sum_{s}\frac{1}{i\omega_s - \omega_{\boldsymbol{p}}}T_{\boldsymbol{\lambda},\boldsymbol{\lambda}}(\boldsymbol{K}, i\omega_n + i\omega_s) \tag{4.5.8}$$

where $\boldsymbol{\lambda} = \frac{1}{2}(\boldsymbol{k} - \boldsymbol{p})$ and $\boldsymbol{K} = \boldsymbol{k} + \boldsymbol{p}$. The dispersion relation[13] for the T-matrix reads

$$T'_{\boldsymbol{\lambda},\boldsymbol{\mu}}(\boldsymbol{K},\omega) = V_{\boldsymbol{\lambda},\boldsymbol{\mu}}(\boldsymbol{K}) + \frac{\mathrm{P}}{\pi}\int_{-\infty}^{+\infty} d\omega'\frac{T''_{\boldsymbol{\lambda},\boldsymbol{\mu}}(\boldsymbol{K},\omega')}{\omega - \omega'} \tag{4.5.9a}$$

where

$$T_{\boldsymbol{\lambda},\boldsymbol{\mu}}(\boldsymbol{K},\omega \pm i\epsilon) = T'_{\boldsymbol{\lambda},\boldsymbol{\mu}}(\boldsymbol{K},\omega) \mp iT''_{\boldsymbol{\lambda},\boldsymbol{\mu}}(\boldsymbol{K},\omega). \tag{4.5.9b}$$

Equations (4.5.9a) and (4.5.9b) may be grouped in the relationship[36]

$$T_{\boldsymbol{\lambda},\boldsymbol{\mu}}(\boldsymbol{K},z) = V_{\boldsymbol{\lambda},\boldsymbol{\mu}}(\boldsymbol{K}) + \frac{1}{\pi}\int_{-\infty}^{+\infty} d\omega' \frac{T''_{\boldsymbol{\lambda},\boldsymbol{\mu}}(\boldsymbol{K},\omega')}{z-\omega'} \tag{4.5.9c}$$

where z is the complex variable $\omega \pm i\epsilon$. By means of Eq. (4.5.9c), the self-energy (4.5.8) becomes

$$\begin{aligned}\Sigma^{(\mathrm{T})}(\boldsymbol{k},i\omega_n) &= \frac{4}{\hbar}\sum_{\boldsymbol{p}} V_{\boldsymbol{\lambda},\boldsymbol{\lambda}}(\boldsymbol{K})\; n_{\boldsymbol{p}}^{(0)} - \frac{4}{\hbar}\sum_{\boldsymbol{p}}\frac{1}{\pi}\int_{-\infty}^{+\infty} d\omega' \; \frac{T''_{\boldsymbol{\lambda},\boldsymbol{\lambda}}(\boldsymbol{K},\omega')}{i\omega_n-\omega'+\omega_{\boldsymbol{p}}} \\ &\quad \times\frac{1}{\beta\hbar}\sum_{s}\left(\frac{1}{i\omega_s-\omega_{\boldsymbol{p}}} - \frac{1}{i\omega_s+i\omega_n-\omega'}\right) \\ &= \frac{4}{\hbar}\sum_{\boldsymbol{p}} n_{\boldsymbol{p}}^{(0)}\left\{V_{\boldsymbol{\lambda},\boldsymbol{\lambda}}(\boldsymbol{K}) + \frac{1}{\pi}\int_{-\infty}^{+\infty} d\omega \frac{T''_{\boldsymbol{\lambda},\boldsymbol{\lambda}}(\boldsymbol{K},\omega')}{i\omega_n-\omega'+\omega_{\boldsymbol{p}}}\right\} \\ &\quad -\frac{4}{\hbar}\sum_{\boldsymbol{p}}\frac{1}{\pi}\int_{-\infty}^{+\infty} d\omega' \frac{T''_{\boldsymbol{\lambda},\boldsymbol{\lambda}}(\boldsymbol{K},\omega')}{i\omega_n-\omega'+\omega_{\boldsymbol{p}}} n(\omega')\end{aligned} \tag{4.5.10}$$

where Eq. (4.2.16) has been used. By means of Eq. (4.5.9c), the self-energy (4.5.1) becomes

$$\Sigma^{(\mathrm{T})}(\boldsymbol{k},\omega_{\boldsymbol{k}} \pm i\epsilon) = \Sigma^{(\mathrm{T})'}(\boldsymbol{k},\omega_{\boldsymbol{k}}) \pm i\Sigma^{(\mathrm{T})''}(\boldsymbol{k},\omega_{\boldsymbol{k}}) \tag{4.5.11}$$

where

$$\begin{aligned}\Sigma^{(\mathrm{T})'}(\boldsymbol{k},\omega_{\boldsymbol{k}}) &= \frac{4}{\hbar}\sum_{\boldsymbol{p}} T'_{\boldsymbol{\lambda},\boldsymbol{\lambda}}(\boldsymbol{K},\omega_{\boldsymbol{k}}+\omega_{\boldsymbol{p}})\; n_{\boldsymbol{p}}^{(0)} \\ &\quad -\frac{4}{\hbar}\sum_{\boldsymbol{p}}\frac{\mathrm{P}}{\pi}\int_{\omega_{\mathrm{bottom}}}^{\omega_{\mathrm{top}}} d\omega' \frac{T''_{\boldsymbol{\lambda},\boldsymbol{\lambda}}(\boldsymbol{K},\omega')}{\omega_{\boldsymbol{k}}+\omega_{\boldsymbol{p}}-\omega'}\; n(\omega')\end{aligned} \tag{4.5.11a}$$

and

$$\Sigma^{(\mathrm{T})''}(\boldsymbol{k},\omega_{\boldsymbol{k}}) = \frac{4}{\hbar}\sum_{\boldsymbol{p}} T''_{\boldsymbol{\lambda},\boldsymbol{\lambda}}(\boldsymbol{K},\omega_{\boldsymbol{k}}+\omega_{\boldsymbol{p}})[n_{\boldsymbol{p}}^{(0)} - n(\omega_{\boldsymbol{k}}+\omega_{\boldsymbol{p}})]. \tag{4.5.11b}$$

In the second term of Eq. (4.5.11a), the restricted integration range is due to the nature of the imaginary part of the T-matrix that is non zero only within the two-magnon band. Moreover, the presence of the Bose factor $n(\omega')$ implies that the temperature dependence of such a term is exponentially small compared to the first one which is proportional to $k^2T^{5/2}$ so that such a term can be neglected. The damping given by Eq. (4.5.11b) leads to two different results according to $\hbar\omega_{\boldsymbol{k}} \ll k_BT$ (long wavelength limit) or $\hbar\omega_{\boldsymbol{k}} \gg k_BT$ (short wavelength): in the first case, the evaluation of the damping[36] reduces to the second order result given by

Eq. (3.6.71). In the second case, the second Bose factor occurring in Eq. (4.5.11b) can be neglected and one recovers the damping given by Eq. (3.6.74). In the low temperature, short wavelength limit, the T-matrix self-energy (4.5.11) becomes

$$\Sigma^{(\mathrm{T})}(\boldsymbol{k}, \omega_{\boldsymbol{k}} \pm i\epsilon) = \frac{4}{\hbar} \sum_{\boldsymbol{p}} T_{\boldsymbol{\lambda},\boldsymbol{\lambda}}(\boldsymbol{K}, \omega_{\boldsymbol{k}} + \omega_{\boldsymbol{p}} \pm i\epsilon) n_{\boldsymbol{p}}^{(0)}. \tag{4.5.12a}$$

Making use of Eqs. (4.5.5) and (4.5.6), the self-energy (4.5.12a) becomes

$$\Sigma^{(\mathrm{T})}(\boldsymbol{k}, \omega_{\boldsymbol{k}} \pm i\epsilon) = -\frac{16J}{\hbar N} \sum_{\boldsymbol{p}} n_{\boldsymbol{p}}^{(0)} \sum_{\alpha\beta} \cos\frac{k_\alpha - p_\alpha}{2} \sin\frac{p_\beta}{2} \sin\frac{k_\beta}{2} \times \left[\mathbf{1} - \frac{1}{2S} \mathbf{B}(\boldsymbol{k} + \boldsymbol{p}, \omega_{\boldsymbol{k}} + \omega_{\boldsymbol{p}} \pm i\epsilon) \right]^{-1}_{\alpha\beta}, \tag{4.5.12b}$$

where the Bose factors appearing in Eq. (4.5.6) have been neglected. We will perform the explicit calculation of the T-matrix at zero temperature in 1D and 3D.

In 1D, an analytic calculation can be performed for any wavevector k. Indeed, the T-matrix of Eq. (4.5.5) reduces to

$$T_{\lambda,\mu}(K, \omega \pm i\epsilon) = -\frac{2J}{N} \frac{\cos\lambda \left(\cos\mu - \cos\frac{K}{2}\right)}{1 - \frac{1}{2S}\mathrm{B}(K, \omega \pm i\epsilon)}. \tag{4.5.13}$$

Using Eq. (3.2.12), one may write Eq. (4.5.6) in the form

$$\mathrm{B}(K, \omega \pm i\epsilon) = \mathrm{B}'(K, x) \pm i\mathrm{B}''(K, x) \tag{4.5.14}$$

where

$$\mathrm{B}'(K, x) = \frac{\mathrm{P}}{\pi} \int_0^\pi d\rho \, \frac{\left(\cos\frac{K}{2} - \cos\rho\right)\cos\rho}{x + \cos\frac{K}{2}\cos\rho} = \left(1 + \frac{x}{\cos^2\frac{K}{2}}\right)\left[1 - xI_0(K, x)\right] \tag{4.5.15}$$

and x is given by Eq. (4.5.7) with $z = 2$. The integral $I_0(K, x)$ appearing in Eq. (4.5.15) is given by[3]

$$I_0(K, x) = \frac{\mathrm{P}}{\pi} \int_0^\pi \frac{d\rho}{x + \cos\frac{K}{2}\cos\rho} = \begin{cases} -\dfrac{1}{\sqrt{x^2 - \cos^2\frac{K}{2}}} & \text{for } x < -\cos\frac{K}{2} \\ 0 & \text{for } -\cos\frac{K}{2} < x < \cos\frac{K}{2} \\ \dfrac{1}{\sqrt{x^2 - \cos^2\frac{K}{2}}} & \text{for } x > \cos\frac{K}{2} \end{cases} \tag{4.5.15a}$$

The imaginary part of $\mathrm{B}(K,x)$ in Eq. (4.5.14) is given by

$$\begin{aligned}\mathrm{B}''(K,x) &= -\int_0^\pi d\rho \cos\rho \left(\cos\frac{K}{2} - \cos\rho\right)\ \delta\left(x + \cos\frac{K}{2}\cos\rho\right) \\ &= \frac{x}{\sqrt{\cos^2\frac{K}{2} - x^2}}\left(1 + \frac{x}{\cos^2\frac{K}{2}}\right) \end{aligned} \tag{4.5.16}$$

for $-\cos\frac{K}{2} < x < \cos\frac{K}{2}$ and zero otherwise. The last row of Eq. (4.5.16) is obtained accounting for the property of the Dirac's δ-function: indeed, its argument vanishes for $\rho = \rho_0 = \arccos(\frac{-x}{\cos K/2})$ only if $|-x/\cos\frac{K}{2}| < 1$. By means of Eqs. (4.5.15) and (4.5.16), Eq. (4.5.14) becomes

$$\mathrm{B}(K,\omega\pm i\epsilon) = \begin{cases} \left(1 + \dfrac{x}{\cos^2\frac{K}{2}}\right)\left(1 + \dfrac{x}{\sqrt{x^2 - \cos^2\frac{K}{2}}}\right) & \text{for } x < -\cos\frac{K}{2} \\ \left(1 + \dfrac{x}{\cos^2\frac{K}{2}}\right)\left(1 \pm i\dfrac{x}{\sqrt{\cos^2\frac{K}{2} - x^2}}\right) & \text{for } -\cos\frac{K}{2} < x < \cos\frac{K}{2} \\ \left(1 + \dfrac{x}{\cos^2\frac{K}{2}}\right)\left(1 - \dfrac{x}{\sqrt{x^2 - \cos^2\frac{K}{2}}}\right) & \text{for } x > \cos\frac{K}{2} \end{cases} \tag{4.5.17}$$

Equations (4.5.13) and (4.5.17) provide the T-matrix for a 1D ferromagnet at zero temperature. Using Eq. (4.5.7), one can see that the first row of Eq. (4.5.17) corresponds to the value of $\mathrm{B}(K,\omega)$ for $\hbar\omega < \hbar\omega_{\mathrm{bottom}} = 8JS(1-\cos\frac{K}{2})$ that is for frequencies below the bottom of the two-spin wave band

$$\hbar\omega_{2\mathrm{sw}} = 4JS\,(1-\cos q_1) + 4JS\,(1-\cos q_2) = 8JS\left(1 - \cos\frac{K}{2}\cos q\right)$$

with $q_1 = \frac{1}{2}K + q$ and $q_2 = \frac{1}{2}K - q$. Indeed, $\hbar\omega_{2\mathrm{sw}}$ is the sum of the energies of two non-interacting spin waves in which K is the wavevector of the complex formed by the two spin waves and q is the relative wavevector of the the pair. The two-spin wave band is the energy region delimited between $\hbar\omega_{\mathrm{bottom}} = 8JS(1-\cos\frac{K}{2})$ and $\hbar\omega_{\mathrm{top}} = 8JS(1+\cos\frac{K}{2})$. The second row of Eq. (4.5.17) corresponds to the value of $\mathrm{B}(K,\omega)$ inside the two-spin wave band $\omega_{\mathrm{bottom}} < \omega < \omega_{\mathrm{top}}$ and the third row corresponds to the value of $\mathrm{B}(K,\omega)$ for $\omega > \omega_{\mathrm{top}}$ that is for frequencies above the band. Note that $\mathrm{B}(K,\omega\pm i\epsilon)$ is a real function outside and a complex function inside the two-spin wave band. Moreover, since $\omega_{\mathrm{bottom}} < \omega_k + \omega_p < \omega_{\mathrm{top}}$, in the self-energy (4.5.12b), one has to select the B-function given by the second row of Eq. (4.5.17) evaluated at $x = -\frac{1}{2}(\cos k + \cos p) = -\cos\frac{k+p}{2}\cos\frac{k-p}{2}$ so that

$$\Sigma^{(\mathrm{T})}(k,\omega_k \pm i\epsilon) = -\frac{16J}{\hbar N}\sum_p n_p^{(0)} \frac{\cos\frac{k-p}{2}\sin\frac{k}{2}\sin\frac{p}{2}}{1 + \frac{1}{S}\frac{\sin\frac{k}{2}\sin\frac{p}{2}}{\cos\frac{k+p}{2}}\left(1 \mp i\frac{\cos\frac{k-p}{2}}{\left|\sin\frac{k-p}{2}\right|}\right)}. \tag{4.5.18}$$

Expanding Eq. (4.5.18) in powers of p and retaining only the main contribution, one has

$$\Sigma^{(\mathrm{T})'}(k,\omega_k) = -\frac{8J}{\hbar N}\sin\frac{k}{2}\sum_p p\ n_p^{(0)}\frac{\cos\frac{k}{2}+\frac{p}{2}\left(1+\frac{1}{S}\right)\sin\frac{k}{2}+O(p^2)}{1+\frac{p}{S}\tan\frac{k}{2}+O(p^2)}$$

$$= -\frac{4J}{\hbar N}\left(1-\frac{1}{S}\right)\sin^2\frac{k}{2}\sum_p p^2\ n_p^{(0)}$$

$$= -\frac{\omega_k}{S}\left(1-\frac{1}{S}\right)\pi\ \zeta\left(\frac{3}{2}\right)\left(\frac{k_BT}{8\pi JS}\right)^{\frac{3}{2}} \tag{4.5.19}$$

for the real part and

$$\Sigma^{(\mathrm{T})''}(k,\omega_k) = \frac{2J}{\hbar SN}\sum_p p^2\ n_p^{(0)}[\sin k + O(p)] = \frac{4J}{\hbar S}\pi\ \zeta\left(\frac{3}{2}\right)\left(\frac{k_BT}{8\pi JS}\right)^{\frac{3}{2}}\sin k \tag{4.5.20}$$

for the imaginary part, where the relationship[3]

$$\frac{1}{N}\sum_p p^2 n_p^{(0)} = \frac{1}{2\pi}\left(\frac{k_BT}{2JS}\right)^{\frac{3}{2}}\int_0^\infty dx\frac{\sqrt{x}}{e^x-1} = 2\pi\ \zeta\left(\frac{3}{2}\right)\left(\frac{k_BT}{8\pi JS}\right)^{\frac{3}{2}}. \tag{4.5.21}$$

has been used. The renormalization (4.5.19) and the damping (4.5.20) of the spin wave frequency for the 1D ferromagnet agree with the renormalization and damping obtained using the method of the equation of motion of the Green function.[37] An interesting feature of the renormalization (4.5.19) is that it is positive (upword renormalization) for $S=\frac{1}{2}$, 0 (at the order $T^{3/2}$) for $S=1$ and negative (downward renormalization) for $S>1$. Moreover, Eq. (4.5.19) points out that only the first two terms of the perturbation expansion contribute to the renormalization at the order $T^{3/2}$ since only terms proportional to 1 and $\frac{1}{S}$ appear in Eq. (4.5.19). Similarly, Eq. (4.5.20) points out that only the term coming from the second-order perturbation expansion contributes to the damping at the order $T^{3/2}$. In particular, only $\Sigma^{(1)}(k)$ and $\Sigma_c^{(2)}(k,\omega_k\pm i\epsilon)$ contribute to the T-matrix of a 1D ferromagnet at the lowest order in temperature. To check this statement, we evaluate directly the first-order term (4.2.16) and the second-order one (4.3.16) for the 1D ferromagnet obtaining

$$\Sigma^{(1)}(\boldsymbol{k}) = -\frac{\omega_k}{2S}\ \frac{1}{N}\sum_p p^2\ n_p^{(0)} = -\pi\ \zeta\left(\frac{3}{2}\right)\ \frac{\omega_k}{S}\left(\frac{k_BT}{8\pi JS}\right)^{\frac{3}{2}} \tag{4.5.22}$$

and

$$\Sigma_c^{(2)'}(k,\omega_k) = \frac{\omega_k}{2S^2}\ \frac{1}{N}\sum_p p^2\ n_p^{(0)} = \pi\ \zeta\left(\frac{3}{2}\right)\ \frac{\omega_k}{S^2}\left(\frac{k_BT}{8\pi JS}\right)^{\frac{3}{2}}, \tag{4.5.23}$$

respectively. Summing Eqs. (4.5.22) and (4.5.23), one recovers the T-matrix result given in Eq. (4.5.19). The third-order term that contributes to the T-matrix is

$\Sigma_d^{(3)'}(k,\omega_k)$ given by Eq. (4.4.17). In 1D, we make the replacements $K=\frac{1}{2}(k+p)$, $\lambda=\frac{1}{2}(k-p)$, $q_1=\frac{1}{2}K+\mu$, $q_3=\frac{1}{2}K-\mu$, $q_2=\frac{1}{2}K+\rho$ and $q_4=\frac{1}{2}K-\rho$, obtaining

$$\Sigma_d^{(3)'}(k,\omega_k)=-\frac{2J}{\hbar S^2}\frac{\mathrm{P}}{N^3}\sum_{\lambda,\mu,\rho}\frac{\cos\lambda(\cos\lambda-\cos\frac{K}{2})}{\cos^2\frac{K}{2}}n^{(0)}_{\frac{1}{2}K-\lambda}$$
$$\times\left\{\left[\frac{1}{N}\sum_{\rho}\frac{\cos\rho(\cos\rho-\cos\frac{K}{2})}{\cos\rho-\cos\lambda}\right]^2\right.$$
$$\left.-\pi^2\left[\frac{1}{N}\sum_{\rho}\cos\rho\left(\cos\rho-\cos\frac{K}{2}\right)\ \delta(\cos\rho-\cos\lambda)\right]^2\right\}. \tag{4.5.24}$$

Using the relationship[3]

$$\frac{\mathrm{P}}{\pi}\int_0^{\pi}d\rho\frac{\cos\rho(\cos\rho-\cos\frac{K}{2})}{\cos\rho-\cos\lambda}=\cos\lambda-\cos\frac{K}{2} \tag{4.5.25a}$$

and

$$\frac{1}{\pi}\int_0^{\pi}d\rho\ \cos\rho\left(\cos\rho-\cos\frac{K}{2}\right)\ \delta(\cos\rho-\cos\lambda)=\frac{1}{\pi}\frac{\cos\lambda\left(\cos\lambda-\cos\frac{K}{2}\right)}{|\sin\lambda|}, \tag{4.5.25b}$$

Equation (4.5.24) becomes

$$\Sigma_d^{(3)'}(k,\omega_k)=-\frac{2J}{\hbar S^2}\ \frac{1}{N}\sum_{\lambda}\frac{\cos\lambda(\cos\lambda-\cos\frac{K}{2})^3}{\cos^2\frac{K}{2}}\left(1-\frac{\cos^2\lambda}{\sin^2\lambda}\right)n^{(0)}_{\frac{1}{2}K-\lambda}. \tag{4.5.26}$$

Replacing K by $k+p$, λ by $\frac{1}{2}(k-p)$ and expanding in powers of p due to the presence of the Bose factor, the main temperature contribution of Eq. (4.5.26) is given by

$$\Sigma_d^{(3)'}(k,\omega_k)=\frac{2J}{\hbar S^2}\ \frac{(2-\cos k)(1+3\cos k)}{1+\cos k}\frac{1}{N}\sum_p p^4\ n_p^{(0)}$$
$$=\frac{2J}{\hbar S^2}\ \frac{(2-\cos k)(1+3\cos k)}{1+\cos k}3\pi^2\ \zeta\left(\frac{5}{2}\right)\left(\frac{k_BT}{8\pi JS}\right)^{\frac{5}{2}} \tag{4.5.27}$$

which is of order $T^{5/2}$ and so it is negligible compared to the terms coming from the first and second-order self-energies of order $T^{3/2}$. The conclusion is that in 1D, the first two terms of the T-matrix expansion give contributions proportional to $\sum_p p^2 n_p^{(0)}$ while from the third term onwards, only contributions of order $\sum_p p^4 n_p^{(0)}$ or higher occur even though all these terms have a single Bose factor. The different powers in p are entered by the function of p that multiplies the Bose factor. In any case, we may check that in the 1D case, the temperature contributions to the self-energy that come from diagrams containing more than one downward line, are of higher order in temperature: to do this, we evaluate explicitly some diagrams that

do not belong to the T-matrix expansion. For instance, the second-order term (4.2.6) corresponding to the diagram $\Sigma_b^{(2)}$ of Fig. 4.2, in 1D reads

$$\Sigma_b^{(2)}(k) = -\frac{3\omega_k}{2S^2}\left[\pi\ \zeta\left(\frac{3}{2}\right)\right]^2\left(\frac{k_BT}{8\pi JS}\right)^3. \tag{4.5.28}$$

The presence of two downward lines in the diagram leads to a contribution proportional to $(T^{3/2})^2 = T^3$ which is the square of the contribution coming from the term with one downward line proportional to $T^{3/2}$. The third-order term (4.4.5) corresponding to the diagram $\Sigma_a^{(3)}$ of Fig. 4.3, in 1D reads

$$\Sigma_a^{(3)}(k) = -\frac{9\omega_k}{4S^3}\left[\pi\ \zeta\left(\frac{3}{2}\right)\right]^3\left(\frac{k_BT}{8\pi JS}\right)^{\frac{9}{2}}. \tag{4.5.29}$$

The three downward lines in the diagram lead to a contribution proportional to $(T^{3/2})^3 = T^{9/2}$ which is the cube of the term containing one downward line. The third-order term (4.4.10) corresponding to the diagram $\Sigma_b^{(3)}$ of Fig. 4.3, in 1D reads

$$\Sigma_b^{(3)}(k) = -\frac{15\omega_k}{8S^3}\left[\pi\ \zeta\left(\frac{3}{2}\right)\right]^3\left(\frac{k_BT}{8\pi JS}\right)^{\frac{9}{2}}. \tag{4.5.30}$$

Again, the three downward lines of the diagram lead to a contribution proportional to $(T^{3/2})^3 = T^{9/2}$. The third-order term (4.4.16) corresponding to the diagram $\Sigma_c^{(3)}$ of Fig. 4.3, in 1D reads

$$\Sigma_c^{(3)}(k) = \frac{2\omega_k}{S^3}\left[\pi\ \zeta\left(\frac{3}{2}\right)\right]^2\left(\frac{k_BT}{8\pi JS}\right)^3. \tag{4.5.31}$$

The presence of two downward lines leads to a contribution proportional to $(T^{3/2})^2 = T^3$. The real part of the third-order term (4.4.24) corresponding to the diagram $\Sigma_f^{(3)}$ of Fig. 4.3, in 1D reads

$$\Sigma_f^{(3)'}(k) = \frac{\omega_k}{4S^3}\left[\pi\ \zeta\left(\frac{3}{2}\right)\right]^2\frac{5\cos k - 1}{1+\cos k}\left(\frac{k_BT}{8\pi JS}\right)^3. \tag{4.5.32}$$

The real part of the third-order term (4.4.27) corresponding to the diagram $\Sigma_g^{(3)}$ of Fig. 4.3, in 1D reads

$$\Sigma_g^{(3)'}(k) = -\frac{3\omega_k}{S^3}\left[\pi\ \zeta\left(\frac{3}{2}\right)\right]^2\left(\frac{k_BT}{8\pi JS}\right)^3. \tag{4.5.33}$$

The expectation that any downward line making a contribution proportional to $T^{3/2}$ in 1D appears to be confirmed. As for the $\frac{1}{S}$-expansion, one can see that any second-order self-energy contribution is proportional to $\frac{1}{S^2}$ as shown by Eqs. (4.5.23) and (4.5.28); any third-order self-energy contribution is proportional to $\frac{1}{S^3}$ as shown by Eqs. (4.5.27) and (4.5.29)–(4.5.33). However, *different* powers in temperature come from terms of the *same* order in $\frac{1}{S}$. This means that $\frac{1}{S}$ is a good perturbation parameter, not the temperature which is, however, the most important expansion parameter to fit experimental data. Moreover, the presence of a single Bose factor, corresponding to diagrams with only one downward line, does not imply (in

1D) that the corresponding temperature contribution is the same at each order of perturbation in $\frac{1}{S}$ since the function that multiplies the Bose factor when expanded in p gives different powers as illustrated when comparing Eqs. (4.5.22) and (4.5.23) with Eq. (4.5.27): all diagrams corresponding to these terms have one downward line as shown in Fig. 4.1 (see $\Sigma^{(1)}$), Fig. 4.2 (see $\Sigma_c^{(2)}$) and Fig. 4.3 (see $\Sigma_d^{(3)}$) but the first two diagrams lead to a contribution proportional to $T^{3/2}$ whereas the third diagram leads to a contribution proportional to $T^{5/2}$. This peculiarity, however, does not apply to 3D systems where any diagram containing one downward line leads to a contribution proportional to $T^{5/2}$. To show this, we evaluate the T-matrix self-energy (4.5.12b) for a 3D lattice. Due to the Bose factor in Eq. (4.5.12b), we can expand the function that multiplies $n_{\boldsymbol{p}}^{(0)}$ in powers of $\boldsymbol{p}$. Then the sum over $\boldsymbol{p}$ in Eq. (4.5.12b) gives non zero contributions only for the even powers of the wavevector $\boldsymbol{p}$, leading to

$$\Sigma^{(\mathrm{T})}(\boldsymbol{k},\omega) = -\frac{16J}{\hbar N}\sum_{\boldsymbol{p}} n_{\boldsymbol{p}}^{(0)}\left\{\sum_{\alpha}\ \frac{1}{4}\ p_\alpha^2 \sin^2\frac{k_\alpha}{2}\left[\mathbf{1}-\frac{1}{2S}\mathbf{B}(\boldsymbol{k},\omega)\right]^{-1}_{\alpha\alpha}\right.$$
$$\left.+\sum_{\alpha,\beta}\ \frac{1}{2}\ p_\beta^2 \cos\frac{k_\alpha}{2}\sin\frac{k_\beta}{2}\left|\frac{\partial}{\partial p_\beta}\left[\mathbf{1}-\frac{1}{2S}\mathbf{B}(\boldsymbol{k}+\boldsymbol{p},\omega)\right]^{-1}_{\alpha\beta}\right|_{\boldsymbol{p}=0}\right\}. \tag{4.5.34}$$

By use of the relationship

$$\left|\frac{\partial}{\partial p_\beta}\left[\mathbf{1}-\frac{1}{2S}\mathbf{B}(\boldsymbol{k}+\boldsymbol{p},\omega)\right]^{-1}_{\alpha\beta}\right|_{\boldsymbol{p}=0}$$
$$=\frac{\partial}{\partial k_\beta}\left[\mathbf{1}-\frac{1}{2S}\mathbf{B}(\boldsymbol{k},\omega)\right]^{-1}_{\alpha\beta}, \tag{4.5.35}$$

Equation (4.5.34) becomes

$$\Sigma^{(\mathrm{T})}(\boldsymbol{k},\omega_{\boldsymbol{k}}\pm i\epsilon) = -\frac{8J}{\hbar}\ \pi\zeta\left(\frac{5}{2}\right)\left(\frac{k_BT}{8\pi JS}\right)^{\frac{5}{2}}\left\{\sum_{\alpha}\sin^2\frac{k_\alpha}{2}\right.$$
$$\times\left[\mathbf{1}-\frac{1}{2S}\mathbf{B}(\boldsymbol{k},\omega_{\boldsymbol{k}}\pm i\epsilon)\right]^{-1}_{\alpha\alpha}+2\sum_{\alpha,\beta}\cos\frac{k_\alpha}{2}\sin\frac{k_\beta}{2}$$
$$\left.\times\left|\frac{\partial}{\partial k_\beta}\left[\mathbf{1}-\frac{1}{2S}\mathbf{B}(\boldsymbol{k},\omega\pm i\epsilon)\right]^{-1}_{\alpha\beta}\right|_{\omega=\omega_{\boldsymbol{k}}}\right\} \tag{4.5.36}$$

where

$$\mathrm{B}_{\alpha\beta}(\boldsymbol{k},\omega_{\boldsymbol{k}}\pm i\epsilon) = \cos\frac{k_\alpha}{2}D_\beta - D_{\alpha\beta} \tag{4.5.37}$$

with

$$D_{\alpha\beta} = \frac{1}{N}\sum_{\boldsymbol{\rho}}\frac{\cos\rho_\alpha\cos\rho_\beta}{\sum_\sigma\cos\frac{k_\sigma}{2}\left(\cos\rho_\sigma-\cos\frac{k_\sigma}{2}\right)\pm i\epsilon} \tag{4.5.37a}$$

and

$$D_\alpha = \frac{1}{N}\sum_{\boldsymbol{\rho}} \frac{\cos\rho_\alpha}{\sum_\sigma \cos\frac{k_\sigma}{2}\left(\cos\rho_\sigma - \cos\frac{k_\sigma}{2}\right) \pm i\epsilon}, \tag{4.5.37b}$$

where $\sigma = x, y, z$. For a SC lattice with $\boldsymbol{k} = (k, k, k)$, one has $D_\alpha = D_1$ for $\alpha = x, y, z$; $D_{\alpha\beta} = D_{11}$ for $\alpha = \beta = x, y, z$; $D_{\alpha\beta} = D_{12}$ for $\alpha \neq \beta$ and the self-energy (4.5.36) becomes

$$\Sigma^{(\mathrm{T})}(k, \omega_k \pm i\epsilon) = -\frac{8J}{\hbar}\,\pi\,\zeta\left(\frac{5}{2}\right)\left(\frac{k_B T}{8\pi JS}\right)^{\frac{5}{2}}\left\{\sin^2\frac{k}{2}\sum_\alpha\left[\mathbf{1} - \frac{1}{2S}\mathbf{B}(k, \omega_k \pm i\epsilon)\right]^{-1}_{\alpha\alpha}\right.$$
$$\left. + 2\cos\frac{k}{2}\sin\frac{k}{2}\sum_{\alpha,\beta}\left|\frac{\partial}{\partial k_\beta}\left[\mathbf{1} - \frac{1}{2S}\mathbf{B}(\boldsymbol{k}, \omega \pm i\epsilon)\right]^{-1}_{\alpha\beta}\right|_{\omega=\omega_k}\right\} \tag{4.5.38}$$

where $\hbar\omega_k = 12JS(1 - \cos k)$. The evaluation of the trace of the inverse matrix of $(\mathbf{1} - \frac{1}{2S}\mathbf{B})$ occurring in the first term of Eq. (4.5.38) is direct: one has

$$\sum_\alpha\left[\mathbf{1} - \frac{1}{2S}\mathbf{B}(k, \omega_k \pm i\epsilon)\right]^{-1}_{\alpha\alpha} = 3\,\frac{1 + \frac{1}{2S}\mathrm{B}_{12}}{1 + \frac{3}{2S}\mathrm{B}_{12}} \tag{4.5.39}$$

where

$$\mathrm{B}_{12} = D_1\cos\frac{k}{2} - D_{12} \tag{4.5.39a}$$

with

$$D_1 = -\frac{1}{3\cos\frac{k}{2}}\alpha(k), \tag{4.5.39b}$$

$$D_{12} = -\frac{1}{3\cos\frac{k}{2}}\frac{1}{N}\sum_{\boldsymbol{\rho}}\frac{\cos\rho_x\cos\rho_y}{\cos\frac{k}{2} - \frac{1}{3}(\cos\rho_x + \cos\rho_y + \cos\rho_z) \mp i\epsilon} \tag{4.5.39c}$$

and

$$\alpha(k) = \frac{1}{N}\sum_{\boldsymbol{\rho}}\frac{\cos\rho_x}{\cos\frac{k}{2} - \frac{1}{3}(\cos\rho_x + \cos\rho_y + \cos\rho_z) \mp i\epsilon}. \tag{4.5.40}$$

As for the second term of Eq. (4.5.38), where the partial derivative with respect to k_β appears, one can proceed as follows

$$\sum_{\alpha,\beta}\left|\frac{\partial}{\partial k_\beta}\left[\mathbf{1} - \frac{1}{2S}\mathbf{B}(\boldsymbol{k}, \omega \pm i\epsilon)\right]^{-1}_{\alpha\beta}\right|_{\omega=\omega_k} = \sum_{\alpha,\beta}\left|\frac{\partial}{\partial k_\beta}\frac{A_{\alpha\beta}}{A}\right|_{k,\omega_k}$$
$$= \left|\frac{1}{A}\sum_{\alpha,\beta}\frac{\partial A_{\alpha\beta}}{\partial k_\beta} - \frac{1}{A^2}\sum_{\alpha,\beta}A_{\alpha\beta}\frac{\partial A}{\partial k_\beta}\right|_{k,\omega_k} \tag{4.5.41}$$

where $A_{\alpha\beta}/A$ and A are the elements and the determinant of the matrix $(\mathbf{1}\text{-}\frac{1}{2S}\mathbf{B})^{-1}$, respectively. The explicit evaluation of the terms appearing in Eq. (4.5.41) gives

$$\left|\frac{1}{A}\sum_{\alpha,\beta}\frac{\partial A_{\alpha\beta}}{\partial k_\beta}\right|_{k,\omega_k} = -\frac{1}{4S}\sin\frac{k}{2}\cos\frac{k}{2}\ \frac{1}{1+\frac{3}{2S}\mathrm{B}_{12}}\left(\sum_{\alpha,\beta}G_{\alpha\beta}-3\sum_{\alpha}G_{\alpha\alpha}\right) \tag{4.5.42}$$

and

$$\begin{aligned}\left|\frac{1}{A^2}\sum_{\alpha,\beta}A_{\alpha\beta}\frac{\partial A}{\partial k_\beta}\right|_{k,\omega_k} &= \frac{1}{4S}\sin\frac{k}{2}\ \frac{1}{1+\frac{3}{2S}\mathrm{B}_{12}}\Bigg[\left(1+\frac{3}{2S}\mathrm{B}_{12}\right)\\ &\quad\times\left(3\ D_1-\cos\frac{k}{2}\sum_{\alpha,\beta}G_{\alpha\beta}\right)\\ &\quad+\sum_{\alpha,\beta}G_{\alpha\alpha\beta}+\frac{1}{2S}\mathrm{B}_{12}\sum_{\alpha,\beta,\gamma}G_{\alpha\beta\gamma}\Bigg].\end{aligned} \tag{4.5.43}$$

D_1 is given by Eq. (4.5.39b),

$$G_{\alpha\beta}=\frac{1}{N}\sum_{\boldsymbol{\rho}}\frac{\cos\rho_\alpha\cos\rho_\beta}{\left[\cos\frac{k}{2}\sum_\sigma\left(\cos\frac{k}{2}-\cos\rho\right)\right]^2}, \tag{4.5.44}$$

$$G_{\alpha\beta\gamma}=\frac{1}{N}\sum_{\boldsymbol{\rho}}\frac{\cos\rho_\alpha\cos\rho_\beta\cos\rho_\gamma}{\left[\cos\frac{k}{2}\sum_\sigma\left(\cos\frac{k}{2}-\cos\rho\right)\right]^2} \tag{4.5.45}$$

and the sum rule $\mathrm{B}_{11}+2\mathrm{B}_{12}=0$ has been used. By means of Eqs. (4.5.39) and (4.5.41)–(4.5.43), Equation (4.5.38) becomes

$$\begin{aligned}\Sigma^{(\mathrm{T})}(k,\omega_k\pm i\epsilon) &= -\frac{8J}{\hbar}\pi\zeta\left(\frac{5}{2}\right)\left(\frac{k_BT}{8\pi JS}\right)^{\frac{5}{2}}\sin^2\frac{k}{2}\Bigg\{3\ \frac{1+\frac{1}{2S}\mathrm{B}_{12}}{1+\frac{3}{2S}\mathrm{B}_{12}}\\ &\quad-\frac{1}{2S}\frac{\cos\frac{k}{2}}{1+\frac{3}{2S}\mathrm{B}_{12}}\Bigg[3\ D_1\left(1+\frac{3}{2S}\mathrm{B}_{12}\right)-\frac{3}{2S}\mathrm{B}_{12}\cos\frac{k}{2}\ \sum_{\alpha,\beta}G_{\alpha\beta}\\ &\quad-3\cos\frac{k}{2}\ \sum_{\alpha}G_{\alpha\alpha}+\sum_{\alpha,\beta}G_{\alpha\alpha\beta}+\frac{1}{2S}\mathrm{B}_{12}\sum_{\alpha,\beta,\gamma}G_{\alpha\beta\gamma}\Bigg]\Bigg\}.\end{aligned} \tag{4.5.46}$$

Finally, using the sum rules

$$\sum_\gamma G_{\alpha\beta\gamma}=\frac{D_{\alpha\beta}}{\cos\frac{k}{2}}+3\ G_{\alpha\beta}\cos\frac{k}{2} \tag{4.5.47}$$

and

$$\sum_\beta D_{\alpha\beta}=3\ D_1\cos\frac{k}{2}, \tag{4.5.48}$$

the T-matrix self-energy (4.5.46) becomes

$$\Sigma^{(\mathrm{T})}(k, \omega_k \pm i\epsilon) = \Sigma^{(1)}(k) Q(k) \tag{4.5.49}$$

where

$$\Sigma^{(1)}(k) = -\frac{\omega_k}{S}\ \pi\ \zeta\left(\frac{5}{2}\right)\left(\frac{k_B T}{8\pi J S}\right)^{\frac{5}{2}} \tag{4.5.49a}$$

is the first-order self-energy,

$$Q(k) = \frac{1 - \frac{1}{2S}B_{12}}{1 + \frac{3}{2S}B_{12}} - \frac{1}{S}D_1 \cos\frac{k}{2} = \frac{1 + \frac{1}{6S}\Gamma(k)}{1 - \frac{1}{2S}\Gamma(k)} + \frac{1}{3S}\alpha(k), \tag{4.5.49b}$$

where $\alpha(k)$ is given by Eq. (4.5.40), and

$$\Gamma(k) = \frac{1}{\cos\frac{k}{2}}\ \frac{1}{N}\sum_{\boldsymbol{\rho}} \frac{\cos\rho_x\left(\cos\frac{k}{2} - \cos\rho_y\right)}{\cos\frac{k}{2} - \frac{1}{3}\left(\cos\rho_x + \cos\rho_y + \cos\rho_z\right) \mp i\epsilon}. \tag{4.5.50}$$

The self-energy (4.5.49) was obtained by Silberglitt and Harris.[36] Notice that unlike the T-matrix self-energy of the LC (1D) given by Eqs. (4.5.19) and (4.5.20), the self-energy of the SC (3D) lattice (4.5.49) consists of an infinite power series in $\frac{1}{S}$. Indeed, Eq. (4.5.49b) may be written as

$$Q(k) = 1 + \frac{\alpha(k)}{3S} + \frac{4}{3}\sum_{n=1}^{\infty}\left[\frac{\Gamma(k)}{2S}\right]^n \tag{4.5.51}$$

showing that all the *infinite* diagrams containing one downward line shown in Fig. 4.4 give the same contribution $T^{5/2}$ in temperature.

Before concluding this section, we evaluate explicitly the real and imaginary part of the self-energy (4.5.49). Let us begin evaluating the real and imaginary part of $\alpha(k)$ and $\Gamma(k)$ given by Eqs. (4.5.40) and (4.5.50). From Eq. (3.2.12), one has

$$\alpha(k) = \alpha'(k) \pm i\alpha''(k) \tag{4.5.52}$$

with

$$\alpha'(k) = \frac{\mathrm{P}}{\pi^3}\int_0^\pi\int_0^\pi\int_0^\pi dx\ dy\ dz \frac{\cos x}{\cos\frac{k}{2} - \frac{1}{3}(\cos x + \cos y + \cos z)}, \tag{4.5.53}$$

$$\alpha''(k) = \frac{1}{\pi^2}\int_0^\pi\int_0^\pi\int_0^\pi dx\ dy\ dz \cos x \quad \delta\left[\cos\frac{k}{2} - \frac{1}{3}\left(\cos x + \cos y + \cos z\right)\right] \tag{4.5.54}$$

and

$$\Gamma(k) = \Gamma'(k) \pm i\Gamma''(k) \tag{4.5.55}$$

with

$$\Gamma'(k) = \alpha'(k) - \frac{\mathrm{P}}{\cos\frac{k}{2}} \frac{1}{\pi^3} \int_0^\pi \int_0^\pi \int_0^\pi dx\ dy\ dz\ \frac{\cos x\ \cos y}{\cos\frac{k}{2} - \frac{1}{3}(\cos x + \cos y + \cos z)}, \tag{4.5.56}$$

$$\Gamma''(k) = \alpha''(k) - \frac{1}{\cos\frac{k}{2}} \frac{1}{\pi^2} \int_0^\pi \int_0^\pi \int_0^\pi dx\ dy\ dz \cos x \cos y \times \delta\left[\cos\frac{k}{2} - \frac{1}{3}(\cos x + \cos y + \cos z)\right]. \tag{4.5.57}$$

The integration over z is direct: indeed, using Eq. (4.5.15a) one has

$$\frac{1}{\pi}\int_0^\pi dz\ \frac{1}{\cos\frac{k}{2} - \frac{1}{3}(\cos x + \cos y + \cos z)} = \begin{cases} -\dfrac{1}{\sqrt{\left[\cos\frac{k}{2} - \frac{1}{3}(\cos x + \cos y)\right]^2 - \frac{1}{9}}} & \text{for } x, y \in D_1 \\ 0 & \text{for } x, y \in D_2 \\ \dfrac{1}{\sqrt{\left[\cos\frac{k}{2} - \frac{1}{3}(\cos x + \cos y)\right]^2 - \frac{1}{9}}} & \text{for } x, y \in D_3 \end{cases} \tag{4.5.58}$$

and

$$\int_0^\pi dz\ \delta\left[\cos\frac{k}{2} - \frac{1}{3}(\cos x + \cos y + \cos z)\right] = \begin{cases} 0 & \text{for } x, y \in D_1 \text{ or } D_3 \\ \dfrac{1}{\sqrt{\frac{1}{9} - \left[\cos\frac{k}{2} - \frac{1}{3}(\cos x + \cos y)\right]^2}} & \text{for } x, y \in D_2 \end{cases} \tag{4.5.59}$$

where the domains D_1, D_2 and D_3 are given by

$$\mathrm{D}_1 : \left\{x, y > 0 | \cos x + \cos y > 1 + 3\cos\frac{k}{2}\right\}, \tag{4.5.60}$$

$$\mathrm{D}_2 : \left\{0 < x, y < \pi | -1 + 3\cos\frac{k}{2} < \cos x + \cos y < 1 + 3\cos\frac{k}{2}\right\} \tag{4.5.61}$$

and

$$\mathrm{D}_3 : \left\{0 < x, y < \pi | \cos x + \cos y < -1 + 3\cos\frac{k}{2}\right\}, \tag{4.5.62}$$

respectively. The domain D_1 exists only if $\cos\frac{k}{2} < \frac{1}{3}$, that is for $k > k_0 = 2\arccos\frac{1}{3} = 0.78365\pi$. The domain D_2 vanishes for $k = 0$ where D_3 extends to the square $0 < x, y < \pi$. In Fig. 4.5a, the domains D_2 and D_3 are shown for $k = \frac{\pi}{2}$. The scenario is qualitatively the same for any k in the range $0 < k < k_0$, where $\mathrm{D}_1 = 0$. On the other hand, the scenario for $k_0 < k < \pi$ is illustrated in Fig. 4.5b

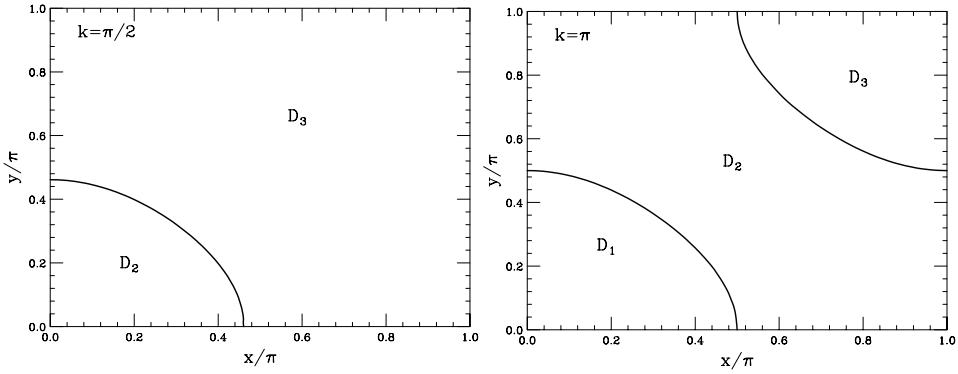

Fig. 4.5. Domains of integration (a) for $k = \frac{\pi}{2}$ (D_2 and D_3) and (b) for $k = \pi$ (D_1, D_2 and D_3).

where the domains D_1, D_2 and D_3 are shown for $k = \pi$. By means of Eqs. (4.5.58) and (4.5.59), Equations (4.5.53), (4.5.54), (4.5.56) and (4.5.57) reduce to

$$\alpha'(k) = \frac{1}{\pi^2}\left\{\iint_{D_3} dx\ dy\ \frac{\cos x}{\sqrt{\left[\cos\frac{k}{2} - \frac{1}{3}(\cos x + \cos y)\right]^2 - \frac{1}{9}}}\right.$$

$$\left. -\theta(k-k_0)\iint_{D_1} dx\ dy \frac{\cos x}{\sqrt{\left[\cos\frac{k}{2} - \frac{1}{3}(\cos x + \cos y)\right]^2 - \frac{1}{9}}}\right\}, \quad (4.5.63)$$

$$\alpha''(k) = \frac{1}{\pi^2}\iint_{D_2} dx\ dy \frac{\cos x}{\sqrt{\frac{1}{9} - \left[\cos\frac{k}{2} - \frac{1}{3}(\cos x + \cos y)\right]^2}}, \quad (4.5.64)$$

$$\Gamma'(k) = \alpha'(k) - \frac{1}{\cos\frac{k}{2}}\ \frac{1}{\pi^2}\left\{\iint_{D_3} dx\ dy\ \frac{\cos x\ cosy}{\sqrt{\left[\cos\frac{k}{2} - \frac{1}{3}(\cos x + \cos y)\right]^2 - \frac{1}{9}}}\right.$$

$$\left. -\theta(k-k_0)\iint_{D_1} dx\ dy\ \frac{\cos x\ \cos y}{\sqrt{\left[\cos\frac{k}{2} - \frac{1}{3}(\cos x + \cos y)\right]^2 - \frac{1}{9}}}\right\} \quad (4.5.65)$$

and

$$\Gamma''(k) = \alpha''(k) - \frac{1}{\cos\frac{k}{2}}\ \frac{1}{\pi^2}\iint_{D_2} dx\ dy \frac{\cos x\ \cos y}{\sqrt{\frac{1}{9} - \left[\cos\frac{k}{2} - \frac{1}{3}(\cos x + \cos y)\right]^2}}, \quad (4.5.66)$$

respectively. The step-function $\theta(k - k_0)$ is 0 for $k < k_0$ and 1 for $k > k_0$. The 2D integrals occurring in Eqs. (4.5.63)–(4.5.66) have to be evaluated numerically. In Fig. 4.6, we show $\alpha'(k)$ (full circles), $\alpha''(k)$ (full squares), $\Gamma'(k)$ (open circles) and $\Gamma''(k)$ (open squares) versus k. Note that $\alpha'(k)$ and $\Gamma'(k)$ are finite at $k = 0$:

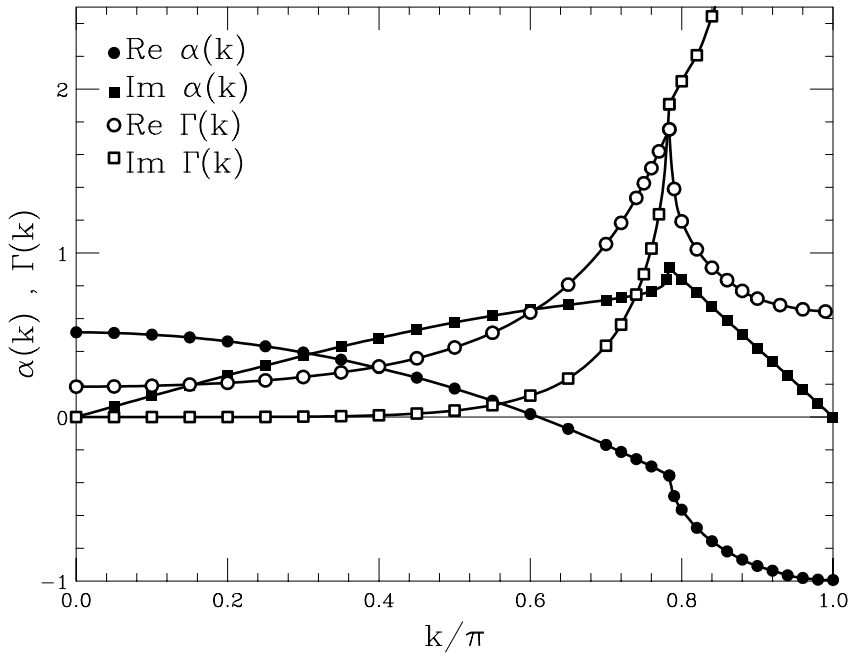

Fig. 4.6. Real part (full circles) and imaginary part (full squares) of $\alpha(k)$; real part (open circles) and imaginary part (open squares) of $\Gamma(k)$ for a SC lattice with $\boldsymbol{k} = (k, k, k)$.

$$\alpha'(0) = \frac{1}{\pi^2}\int_0^\pi \int_0^\pi dx\ dy\ \frac{\cos x}{\sqrt{\left[1 - \frac{1}{3}\left(\cos x + \cos y\right)\right]^2 - \frac{1}{9}}} = 0.51639 \qquad (4.5.67)$$

and

$$\Gamma'(0) = \alpha'(0) - \frac{1}{\pi^2}\int_0^\pi \int_0^\pi dxdy \frac{\cos x\ cosy}{\sqrt{\left[1 - \frac{1}{3}\left(\cos x + \cos y\right)\right]^2 - \frac{1}{9}}}$$

$$= 0.18524. \qquad (4.5.68)$$

On the contrary, $\alpha''(k)$ and $\Gamma''(k)$ vanish at $k = 0$. In particular, in the limit $k \to 0$, the domain D_2 reduces to the quarter of the circle $x^2 + y^2 < \frac{3}{4}k^2$ with $x, y > 0$, so that

$$\alpha''(k \to 0) \simeq \frac{3}{\pi^2}\int_0^{\frac{\pi}{2}} d\theta \int_0^{\frac{\sqrt{3}}{2}k} qdq \frac{1}{\sqrt{\frac{3}{4}k^2 - q^2}} = \frac{3\sqrt{3}}{4\pi}k \qquad (4.5.69)$$

and $\Gamma''(k \to 0)$ vanishes with a power higher than k^3. Both the linear dependence on k of $\alpha''(k)$ and the flatness of the function $\Gamma''(k)$ for $k \to 0$ are clearly seen

in Fig. 4.6. At the zone corner (ZC), that is for $k = \pi$, one has $\alpha'(\pi) = -1$ and $\alpha''(k \to \pi) \simeq 4.21(1 - \frac{k}{\pi})$. The divergence of $\Gamma''(k)$ for $k \to \pi$ is caused by the factor $\frac{1}{\cos(k/2)}$ in Eq. (4.5.66). Indeed, for $k \to \pi$, $\Gamma''(k)$ diverses as $0.37(1 - \frac{k}{\pi})^{-1}$. However, $\Gamma'(\pi)$ is finite since the integrals occurring in Eq. (4.5.65) become equal at $k = \pi$, balancing the divergence entered by the factor $\frac{1}{\cos(k/2)}$ and leading to $\Gamma'(\pi) \simeq 0.64$. Fig. 4.6 shows that the arise of the domain D_1 at $k = k_0$ leads to a cusp in both α and Γ.

The real and imaginary parts of $Q(k)$ given by Eq. (4.5.49b) become

$$Q'(k) = \frac{\left[1 + \frac{1}{6S}\Gamma'(k)\right]\left[1 - \frac{1}{2S}\Gamma'(k)\right] - \frac{1}{12S^2}\Gamma''(k)^2}{\left[1 - \frac{1}{2S}\Gamma'(k)\right]^2 + \frac{1}{4S^2}\Gamma''(k)^2} + \frac{1}{3S}\alpha'(k) \tag{4.5.70}$$

and

$$Q''(k) = \frac{\frac{2}{3S}\Gamma''(k)}{\left[1 - \frac{1}{2S}\Gamma'(k)\right]^2 + \frac{1}{4S^2}\Gamma''(k)^2} + \frac{1}{3S}\alpha''(k), \tag{4.5.71}$$

respectively. As one can see from Eqs. (4.5.70) and (4.5.71), $Q(k)$ is S-dependent. In Fig. 4.7, we show the real and imaginary part of $Q(k)$ vs k for several spin values. In the long wavelength limit one has

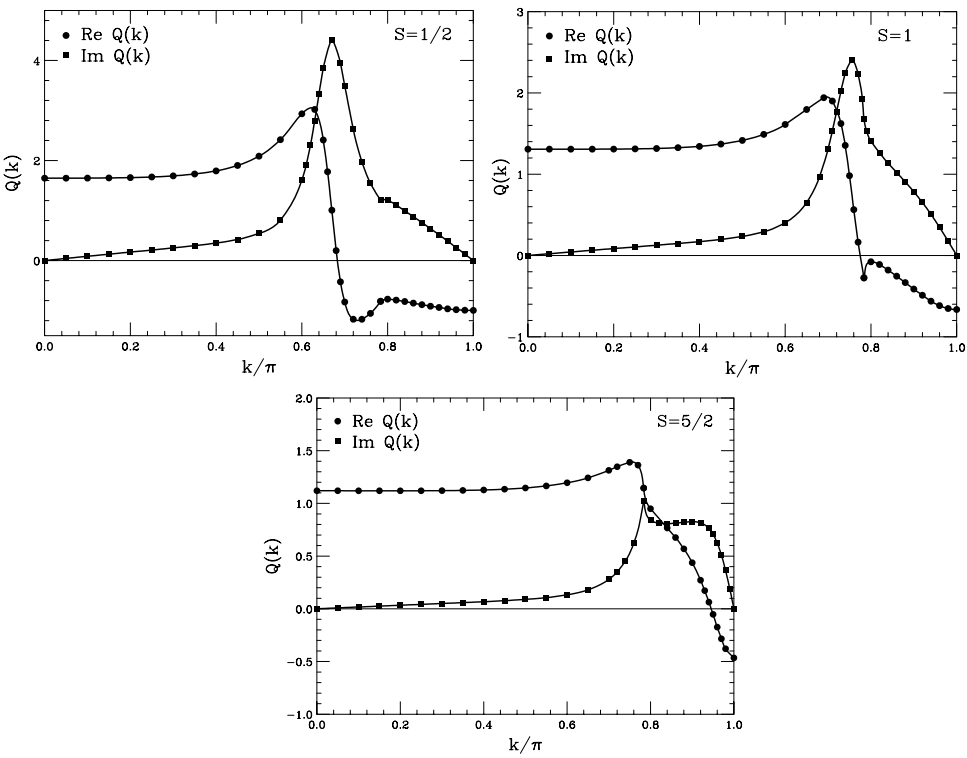

Fig. 4.7. Real (full circles) and imaginary (full squares) parts of $Q(k)$ for $S = 1/2$, 1 and 5/2.

$$Q'(0) = \frac{1 + \frac{1}{6S}\Gamma'(0)}{1 - \frac{1}{2S}\Gamma'(0)} + \frac{\alpha'(0)}{3S} = \frac{1 + 0.03087/S}{1 - 0.09262/S} + \frac{0.17213}{S} \tag{4.5.72a}$$

and

$$Q''(k \to 0) = \frac{\alpha''(k \to 0)}{3S} = \frac{|\boldsymbol{k}|}{4\pi S} + O(k^3). \tag{4.5.72b}$$

For $k \to \pi$, one obtains

$$Q'(k \to \pi) = -\frac{S+1}{3S} \tag{4.5.73a}$$

and

$$Q''(k \to \pi) = 0. \tag{4.5.73b}$$

Note that $Q'(k)$ changes its sign going from $k = 0$ to $k = \pi$ for any S as shown in Fig. 4.7. For $S = 1/2$ and $S = 1$, $Q''(k)$ shows a maximum located very close to the value of k at which $Q'(k)$ changes its sign: $k = 0.683\pi$ and 0.775π for $S = 1/2$ and 1, respectively. The real part (renormalization) and the imaginary part (damping) of the T-matrix self-energy are given by

$$\Sigma^{(\mathrm{T})'}(k, \omega_k) = \Sigma^{(1)}(k)\ Q'(k) \tag{4.5.74}$$

and

$$\Sigma^{(\mathrm{T})''}(k, \omega_k) = -\Sigma^{(1)}(k)\ Q''(k) \tag{4.5.75}$$

with

$$\Sigma^{(1)}(k) = -0.18064\ \frac{J}{\hbar}\left(\frac{k_B T}{2JS}\right)^{\frac{5}{2}} \sin^2\frac{k}{2}. \tag{4.5.76}$$

In Fig. 4.8, the renormalization (full circles) and damping (full squares) of the spin wave with $S = 1/2$ are shown together with the first-order result (full stars). Fig. 4.8 coincides with Fig. 2 of Silberglitt and Harris[36] except for a factor 2 due to a different choice of the scale. Note that the T-matrix renormalization seems to agree with the first-order result for $k \to 0$. However, for small k, one has

$$\Sigma^{(\mathrm{T})'}(k \to 0) = -\frac{2J}{\hbar}\ \pi\ \zeta\left(\frac{5}{2}\right)\left(\frac{k_B T}{8\pi JS}\right)^{\frac{5}{2}} |\boldsymbol{k}|^2 \left(\frac{1 + 0.03087/S}{1 - 0.09262/S} + \frac{0.17213}{S}\right) \tag{4.5.77}$$

so that Eq. (4.5.77) is in accord with the first-order result as regards the powers $k^2 T^{5/2}$ but the coefficient (1.6474, for $S = 1/2$) recovers the first-order result (1, for any S) only for $S \to \infty$. As k increases, the difference between the first-order result (full stars) and the T-matrix renormalization (full circles) appears more and more marked up to become dramatic close to the ZC where the first-order and the T-matrix renormalization have opposite signs. For k small enough, while respecting

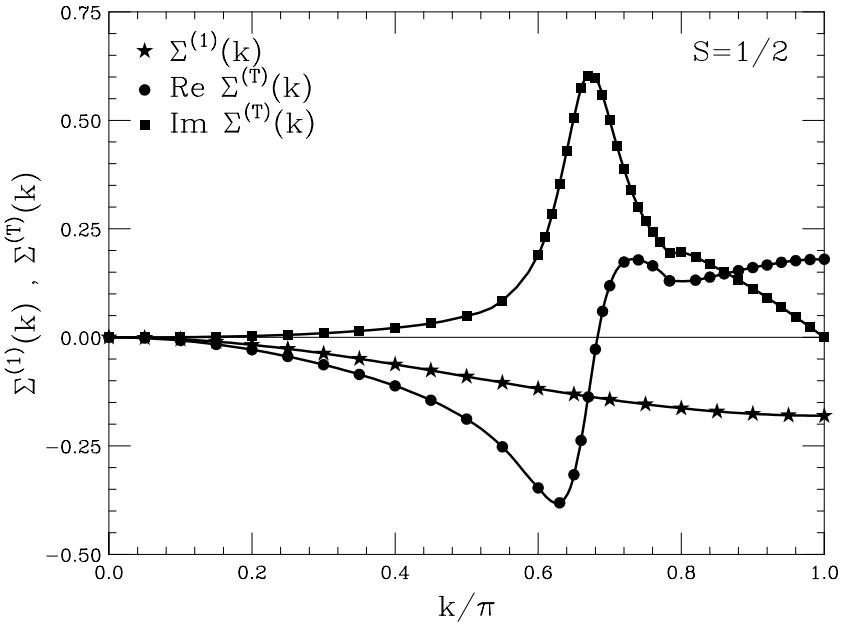

Fig. 4.8. First-order self energy $\Sigma^{(1)}$ (stars), real (full circles) and imaginary (full squares) part of the T-matrix self-energy $\Sigma^{(\mathrm{T})}$ for a SC lattice with $\boldsymbol{k} = (k, k, k)$ and $S = 1/2$ in units of $\frac{J}{\hbar}\left(\frac{k_B T}{2JS}\right)^{5/2}$.

the inequality $\hbar\omega_k \gg k_B T$, as the basis of the calculations of this section, the damping given by Eq. (4.5.75) reduces to

$$\Sigma^{(\mathrm{T})''} \simeq \frac{J}{2\hbar S}\,|\boldsymbol{k}|^3\,\zeta\left(\frac{5}{2}\right)\left(\frac{k_B T}{8\pi JS}\right)^{\frac{5}{2}} \tag{4.5.78}$$

that coincides with the second-order result given by Eq. (3.6.82). Figure 4.8 shows a resonant-like behaviour at $k = 0.683\pi$ that can be traced back to the cross between the renormalized and damped spin wave with the two-magnon (damped) bound state inside the two-spin wave band.[36] For $k > 0.683\pi$, the renormalization becomes positive. This fact is understood as a repulsion between the single particle excitation and the bound states.[36]